COMMUNITY COMPOSITION OF NITRITE REDUCTASE GENES IN AN ACID MINE DRAINAGE ENVIRONMENT

by

BEN WISE

B.A., University of Colorado, 2013.

A thesis submitted to the

Faculty of the Graduate School of the

University of Colorado in partial fulfillment

of the requirements for the degree of

Master of Science

Environmental Science Program

2017

This thesis for the Master of Science degree by

Ben R. Wise

has been approved for the

Environmental Science Program

by

Annika C. Mosier, Chair

Christy Briles

Timberley M. Roane

Date: July 29, 2017

Wise, Ben (M.S. Environmental Science)

Community Composition of Nitrite Reductase Genes in an Acid Mine Drainage Environment

Thesis directed by Assistant Professor Annika C. Mosier

ABSTRACT

High elevation, mountainous regions have a high concentration of mining activities and resulting acid mine drainage (AMD) that is typically acidic and often contains elevated concentrations of metals. The impacts of AMD on denitrifying microbial communities is not well understood, despite these organisms' central role in the nitrogen cycle, contribution to greenhouse gas production, and potential to provide ecosystem services through the mitigation of nitrogen pollution. This study examined denitrifying microbes across four regions within the Iron Springs Mining District (13 sites over four time-points) located in Southwest Colorado at high elevation that receive AMD or naturally-occurring acid rock drainage (ARD). Denitrification functional gene sequences (*nirS* and *nirK* coding for nitrite reductase) had a high number of observed OTUs (260 for *nirS* and 253 for *nirK*) and were observed at sites with pH as low as 3.2, dissolved oxygen as low as 1.0 mg/L, and metals >10 mg/L (including aluminum, iron, manganese, and zinc). A majority of the *nirK* and *nirS* OTUs (>60%) were present in only one sampling region. Approximately 8% of the *nirK* and *nirS* OTUs had a more cosmopolitan distribution with presence in three or more regions. Phylogenetically related OTUs were found across sites with very different chemistry. The total *nirS* community structure was correlated to iron, conductivity, sodium, and calcium, which may suggest that these factors play an important role in shaping the *nirS* community. Overall, these findings improve upon our understanding of the potential for denitrification within an ecosystem impacted by AMD and provide a foundation for future research to understand the rates and physiology of these denitrifying organisms.

The form and content of this abstract are approved. I recommend its publication.

Approved: Annika C. Mosier

ACKNOWLEDGEMENTS

I cannot fully express my appreciation for the guidance, patience, and fortitude that Dr. Annika C. Mosier has provided throughout the duration of this project. I am tremendously thankful for the opportunity she has given me to work alongside her. I would also like to thank my thesis committee members: Dr. Christy Briles for being both a friend and mentor and Dr. Timberley M. Roane for her unaltering enthusiasm and willingness to help.

I am thankful to Robert Edgar, Adrienne Narrowe, Bhargavi Ramanathan, and Sladjana Subotic for support on bioinformatics analysis. I would like to thank Joshua D. Sackett and Ashley Joslin for sample collection. I would like to thank the following institutes for their role in biological and chemical analyses: United States Environmental Protection Agency Region 8 Laboratory, and the Roy J. Carver Biotechnology Center at the University of Illinois.

As with all of my accomplishments, past and future, I must thank my family. I owe my patience, inquisitiveness, and work ethic to my parents, John and Carol Wise. I owe my confidence and passion to my sister, Madeline Wise. I love you guys.

TABLE OF CONTENTS

LIST OF TABLES

LIST OF FIGURES

CHAPTER 1

BACKGROUND

Denitrifying microbes perform an important ecosystem service in the conversion of nitrate to nitrogen gas (Eq. 1) (Seitzenger et al., 2006). Denitrifiers can help to limit eutrophication and play an integral in the nitrogen cycle. At the global scale, denitrification controls most of the fixed nitrogen in the world's oceans, which in turn regulates primary production and dissolved CO_2 in the oceans and atmosphere (Altabet et al., 2002). The process of denitrification also affects global climate through the production of nitrous oxide (N_2O); an important greenhouse gas.

Eq. 1: $NO_3^- \rightarrow NO_2^- \rightarrow NO \rightarrow N_2O \rightarrow N_2$

Denitrification involves four enzymatically-catalyzed steps (Fig. 1): nitrate reduction, nitrite reduction, nitric oxide reduction, and nitrous oxide reduction (Philippot et al. 2002). These four steps are catalyzed by separated enzymes (Nar, Nir, Nor, and Nos). Although denitrification is classified as a type of anaerobic respiration (typically coupled to the oxidation of organic matter in the absence of oxygen), denitrifying bacteria have been shown to reduce nitrate to nitrogen gases under low oxygen conditions, typically less than ~0.2 mg O_2 per liter (Seitzinger et al., 2006). Thus, denitrification occurs under conditions when O_2 supply as a respiratory electron acceptor is limited.

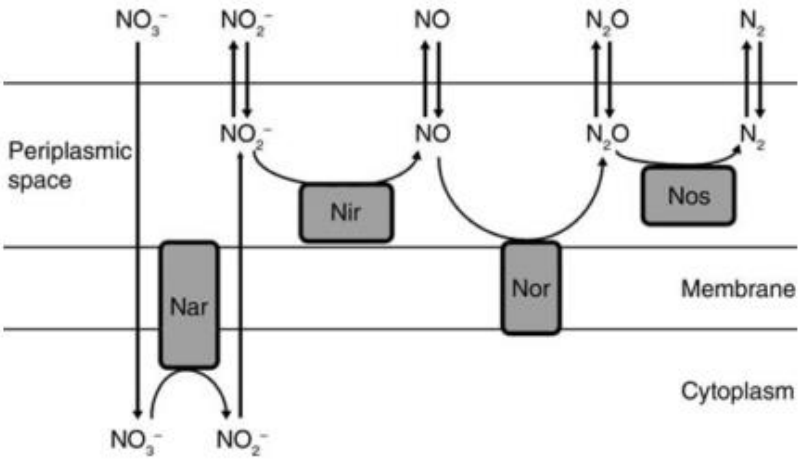

Figure 1. Sequential reductive pathway of denitrification showing the location of enzymes relative to the cytoplasmic membrane. Nar, nitrate reductase; Nir, nitrite reductase; Nor, nitric oxide reductase; Nos, nitrous oxide reductase (Wallenstein et al., 2006).

The nitrite reduction step of denitrification is unique among other forms of nitrate metabolism (Shapleigh, 2006). Nitrite reductase is an especially important enzyme in the denitrification process because it catalyzes the first committed step to a gaseous product through the reduction of nitrite to nitric oxide (Zumft, 1997). This protein occurs in two separate and evolutionarily unrelated forms: *NirK* (containing copper) and *NirS* (containing iron). Characterizing communities of denitrifying microorganisms is most often accomplished through analysis of the *nirS* and *nirK* denitrification functional genes as opposed to 16S rRNA genes because denitrifiers are found within a wide range of phylogenetically unrelated groups from over 50 genera (Zumft, 1997). Nitrite reductase genes have been studied in a plethora of environments, not including those that have been affected by acid mine drainage (AMD), despite this being a widespread pollutant.

AMD is a well-documented type of freshwater pollutant. The waters that drain from active and abandoned mines are typically acidic and often contain elevated concentrations of metals. The acidic and metal-rich fluids that characterize AMD are generated by the chemical weathering of rocks that contain metal sulfides, such as pyrite (FeS_2), arsenopyrite (FeAsS), chalcopyrite

($CuFeS_2$), sphalerite (ZnS), and marcasite (FeS_2) (Baker and Banfield, 2003). The generation of AMD begins with the oxidation of ferrous iron by oxygen (Eq. 1). Ferric iron is then reduced by a sulfide such as pyrite (Eq. 2). The overall reaction results in dissolved ferrous iron, sulfate, and hydrogen ions (Eq. 3). The oxidation of sulfide mineral may initially be abiotic but the rate of the reaction is increased by the presence of prokaryotes through the regeneration of ferric iron via ferrous iron oxidation (Johnson and Hallberg, 2005) (Eq. 4).

$$(1) \quad Fe^{2+} + 3.5O_2 + 14H^+ = 14Fe^{3+} + 7H_2O$$

$$(2) \quad FeS_2 + 14Fe^{3+} + 8H_2O = 15Fe^{2+} + 2SO_4^{2-} + 16H^+$$

$$(3) \quad FeS_2 + 3.5O_2 + H_2O = Fe^{2+} + 2SO_4^{2-} + 2H^+$$

$$(4) \quad 4Fe^{2+} + O_2 + 4H^+ \rightarrow 4Fe^{3+} + 2H_2O$$

Pyrite-rich earth is often mined for other metals such as gold (Au), silver (Ag), copper (Cu), zinc (Zn), and lead (Pb), which are released during the oxidation of metal sulfide (Baker and Banfield, 2005). Iron, in either ferrous or ferric forms is the dominant metal present in AMD (Johnson and Hallberg, 2005). Metals within AMD systems have widespread, nonspecific biological toxicities and their effects on ecosystems are poorly understood. Metals and metalloids can be divided into two categories: essential metals required in some unicellular metabolisms (e.g., Co, Cu, Mn, and Zn) and toxic metals with no known essential functions (e.g. As, Cd, Hg, Pb, and U). The negative effects of these metals include cell membrane disruption, disabled DNA replication, stunted growth in plants, and neurological impairment, cancer, and organ failure in animals (Roane and Lantz, 2016). Acidity (pH <6) often increases the quantity of dissolved metals in solution, while adsorption and precipitation reactions increase with pH >7. Organic matter also influences solubility by binding to metals and thus reducing the solubility.

Mining within the study area analyzed here, the Iron Springs Mining District, began in the mid 1870's. Mainly silver ore was packed over the Ophir Pass to a smelter at Silverton.

Development of the town of Ophir, CO (in the Southwestern corner of the state, approximately 5.5 miles South of Telluride) proceeded at a steady pace until 1890 when the railroad reached the town and electricity was made widely available through the construction of a local power plant. Residents quickly flocked to Ophir in search of the silver and low-grade gold that was abundant in the veins straddling either side of the town and Howard Fork River. Records of the amount of ore removed are very rare. The only formal report is for 1883, when 18 mines within the district produced 96,500 oz of silver and 760,000 lbs of lead (Luedke, 1996). By 1920, the heavy assault on the mines left them devoid of valuable ore except for that existing deep into the vein systems, yet extracting this ore was outside the expertise of the local miners. By 1947, most of the mines and mills had fallen into disrepair (Neubert et al., 2002). Documentation does not exist for most of the mines and mills within the Iron Springs Mining District (Luedke, 1996).

This research was undertaken to assess the overall community structure of nitrite reductase genes in an AMD environment and to look for relationships between community structure and environmental variables. Both *nirK* and *nirS* groups had high numbers of observed OTUs (253 for *nirK* and 260 for *nirS*) that were phylogenetically diverse. The *nirS* community had a significant relationship to iron, sodium, calcium, and conductivity. Both *nirK* and *nirS* communities showed potential adaptability to very acidic conditions. Future work should continue to investigate the relationship between nitrite reductase genes and environmental variables at smaller spatial scales. For instance, within the New Dominion region, how might the CSIB community differ from other sites? Future work should also assess rates of denitrification in this environment. Potential Nir adaptability to high iron concentrations should be addressed in an incubation study. Ultimately, this research has applicability to industry; denitrifiers that are adapted to harsh conditions may be utilized to treat specialized industrial waste.

CHAPTER 2

INTRODUCTION

Nitrogen is an essential element required by all life on Earth, mainly for the synthesis of amino acids and nucleotides. Nitrogen availability is controlled by the balance between the microbiologically-driven processes of nitrogen fixation (atmospheric $N_2 \rightarrow NH_4^+$), nitrification ($NH_4^+ \rightarrow NO_3^-$), and anammox/denitrification that recycles fixed nitrogen back into atmospheric N_2 (Canfield et al., 2010). Denitrification involves four enzymatically-catalyzed steps: nitrate reduction by *Nar* proteins, nitrite reduction by *Nir* proteins, nitric oxide reduction by *Nor* proteins, and nitrous oxide reduction by *Nos* proteins (Philippot et al., 2002). The nitrite reduction step of denitrification catalyzes the first committed step to a gaseous product through the reduction of nitrite to nitric oxide (Zumft, 1997). The *Nir* protein occurs in two separate and evolutionarily unrelated forms: *NirK* (utilizing copper) and *NirS* (utilizing iron).

Due to their abundance and ubiquity across natural environments, denitrifiers have proven to be one of the most successful physiological groups of microorganisms (Shapleigh, 2013). Despite this, little is known about denitrification in systems impacted by acid mine drainage (AMD), which is characterized by acidic and metal-rich fluids generated by the weathering of rocks that contain metal sulfides. Sediment denitrification in several AMD-impacted streams in Colorado (pH 2.6-6.0) was readily induced in the presence of nitrate (Baesman et al., 2006). However, it is unknown whether this is a general phenomenon in other AMD-impacted systems, whether the denitrifier community may be influenced by specific environmental conditions that characterize AMD systems, or if different denitrifying organisms (e.g., *nirK*- and *nirS*-type denitrifiers) respond differently within this harsh environment.

While the impacts of AMD on denitrification are largely unknown, other research has evaluated how specific factors associated with AMD influence denitrifier communities. For example, acidic pH has repeatedly been shown to be a limiting factor in both diversity and rates of denitrification (Mendez-Garcia et al., 2015; Wallenstein et al., 2006; Simek et al., 2002; Wiljer and Delwiche, 1954). Nonetheless, denitrifier communities within environments that are historically acidic may be well-adapted to these conditions and maintain activity at low pH (Parkin et al., 1985; Di Capua et al., 2017). Previous studies have also shown that heavy metals are an important factor in shaping denitrifier community composition in soils contaminated with heavy metals (Kandeler et al., 1996; Holtan-Hartwig et al., 2002; Cao et al., 2008). As the concentration of heavy metals increases, the diversity of denitrifiers and rates of denitrification generally decrease (Sobolev and Begonia, 2008; Liu et al., 2016).

In the present study, we used high-throughput sequencing to examine the diversity and changes in relative abundance of nitrite reductase genes in AMD-impacted sediments in the Colorado Rocky Mountains. AMD poses a significant environmental threat in Colorado due to the ubiquity of abandoned mines (~23,000), many of which continuously emit AMD into freshwater systems (Colorado Geological Survey, 1998). The objectives of this study were to assess the overall community structure of *nirK* and *nirS* gene sequences and to determine if community structure corresponded to environmental variables. Approximately 8% of the *nirK* and *nirS* OTUs had a cosmopolitan distribution across sites with wide ranging pH and metal concentrations, possibly suggesting that these organisms are tolerant of variable conditions. Iron and conductivity appeared to play a role in shaping the overall *nirS* community composition. Ultimately, gaining a better understanding of how denitrifying microbes respond to adverse environmental conditions may improve our ability to maximize their conversion of nitrate to nitrogen gas—an important ecosystem service.

CHAPTER 3

MATERIALS AND METHODS

Site Description and Sample Collection

The Iron Springs Mining District located in Ophir, Colorado consists of several abandoned mines. From 1877-1960, the Iron Springs Mining District was predominantly mined for metals such as silver, gold and lead, and to some extent for iron and tungsten (Nash, 2002). AMD from these mines continues to drain directly into the Howard Fork River. The mining district was divided into four regions for sampling based on the proximity of individual sample sites within each region and their unique environmental conditions: Caribbeau, New Dominion, Iron Bog, and Howard Fork River.

Sampling, measurement of environmental parameters, DNA extraction, and amplicon sequencing were performed as described previously (Ramanathan, 2016; Sackett, 2015). Composite sediment samples (approximately two inches deep) were collected from 13 sampling sites during June and August 2013 and from 11 sampling sites during June and September 2014 at Iron Springs. Samples were stored on dry ice in the field until permanent storage at -20˚C in the laboratory freezer. For total recoverable metal analysis (TRW), 500 mL of surface water sample was collected, acidified to pH <2 with concentrated nitric acid and stored at 4˚C. For dissolved metal analysis (DM), 500 mL of surface water sample was collected, filtered with a cellulose nitrite membrane filter (Thermo Scientific, Waltham, MA), acidified to pH <2 with concentrated nitric acid and stored at 4˚C.

Environmental Parameters

Temperature, pH, conductivity, and dissolved oxygen were measured at the sediment surface using a Thermo Scientific Orion 5-Star Multiparameter Meter Kit (Thermo Fisher

Scientific, Inc., Waltham, MA) and an *In-Situ* Multiparameter meter. Total recoverable and dissolved metal concentration analysis of the Iron Springs water samples were done at the EPA Region 8 lab (Golden, CO) using Inductively-coupled Plasma Mass Spectrometry (ICP-MS) following EPA method 200.8, and Inductively-coupled Plasma Optical Emission Spectrometry (ICP-OES) following EPA method 200.7. The analytes measured for the total recoverable metal concentrations (TRW) and dissolved metal concentrations (DM) included aluminum (Al), antimony (Sb), arsenic (As), barium (Ba), cadmium (Cd), calcium (Ca), copper (Cu), iron (Fe), lead (Pb), magnesium (Mg), manganese (Mn), nickel (Ni), selenium (Se), silver (Ag), sodium (Na), strontium (Sr), thallium (Tl), vanadium (V) and zinc (Zn).

DNA Extraction and Amplicon Sequencing

The MO-BIO PowerMax Soil DNA Isolation Kit (MO BIO Laboratories, Inc., Carlsbad, CA) was used to isolate total DNA from subsamples (~10 grams) of mechanically homogenized saturated composite sediment from each sample site. DNA extracts were quantified using the Qubit dsDNA HS Assay Kit with the Qubit 2.0 Fluorometer (Life Technologies Corporation, Carlsbad, CA). High quality samples (n=38) based on gel electrophoresis, DNA quantification, and PCR amplification were selected for further analyses (excluded samples were Carib01Jun14, FenND03Jun13, and all samples from sites Opp03, NDGP, and NDCS02). DNA extracts from each sample were sent to the University of Illinois Roy J. Carver Biotechnology Center, Urbana, Illinois for amplicon sequencing on the Illumina MiSeq sequencing platform. Library preparation was completed with the Fluidigm 48.48 Access Array IFC platform (Fluidigm Corporation, South San Francisco, CA) to amplify the *nirK* and *nirS* genes using the PCR primer sets nirK876/nirK1040 (Henry et al., 2004) and nirSCd3aF/nirSR3cd (Kandeler et al., 2006; Throbäck et al., 2004), respectively.

Table 2.1: List of PCR primers used for amplicon sequencing, including primer sequence and expected region and size of amplification.

Gene	Forward Primer	Reverse Primer	Fragment Size	Reference
Denitrification *nirS*	nirSCd3aF (5'-AACGYSAAGGARACSGG)	nirSR3cd (5'-GASTTCGGRTGSGTCTTSAYGAA)	425 bp	(Kandeler et al., 2006; Throbäck, Enwall, Jarvis, & Hallin, 2004)
Denitrification *nirK*	nirK876 (5'-ATYGGCGGVCAYGGCGA)	nirK1040 (5'-GCCTCGATCAGRTTRTGGTT)	165 bp	(Henry et al., 2004)

Samples were diluted to a final concentration of 2 ng/μL. A mastermix was prepared with Roche (Basel, Switzerland) High Fidelity Fast Start Kit and 20x Access Array loading reagent according to Fluidigm protocols. Into each well of a PCR plate, 1 μL of each sample was mixed with 1 μL of Fluidigm Illumina linkers and unique barcodes mix, 0.5 μL of 10X FastStart Reaction Buffer without $MgCl_2$, 0.9 μL of 25 mM $MgCl_2$, 0.25 μL of DMSO, 0.1 μL of 10 mM PCR grade nucleotide mix, 0.05 μL of 5 U/μL FastStart High Fidelity enzyme blend, 0.25 μL of 20X Access Array Loading Reagent, and 0.95 μL of water. In a separate plate, 20X primer solutions were prepared by adding 2 μL of each forward and reverse primer (synthesized by IDT Corp, Coralville, IA), 5 μL of 20X Access Array Loading Reagent, and 91 μL of water.

Once the sample mixture was complete, 4 μL was loaded into the sample inlets and 4 μL of the primer solution was loaded into the primer inlets of a primed Fluidigm 48.48 Access Array IFC. The IFC was then placed in a Fluidigm AX controller for microfluidic mixing of each primer and sample combination before being loaded into the Fluidigm Biomark HD PCR machine. Amplicons were generated using the following Access Array cycling program without imaging: 50°C for 2 minutes, 70°C for 20 minutes, 95°C for 10 minutes, 10 cycles of (95°C for 15 seconds, 60°C for 30 seconds, and 72°C for 1 minute), 2 cycles of (95°C for 15 seconds, 80°C for 30

seconds, 60°C for 30 seconds, and 72°C for 1 minute), 8 cycles of (95°C for 15 seconds, 60°C for 30 seconds, and 72°C for 1 minute), 2 cycles of (95°C for 15 seconds, 80°C for 30 seconds, 60°C for 30 seconds, and 72°C for 1 minute), 8 cycles of (95°C for 15 seconds, 60°C for 30 seconds, and 72°C for 1 minute) and 5 cycles of (95°C for 15 seconds, 80°C for 30 seconds, 60°C for 30 seconds, and 72°C for 1 minute).

After amplification, 2 μL of Fluidigm Harvest Buffer was added to each sample inlet, and the IFC loaded onto the AX controller to harvest all PCR products from each sample (e.g., all primer amplifications pooled together for each sample). The PCR products were quantified using Qubit and stored at -20°C. The samples were run on a Fragment Analyzer (Advanced Analytics, Ames, IA) to confirm the expected sizes of amplicons. All of the 48 samples (containing all primer amplifications pooled together) were then pooled together in equal DNA concentrations into one tube. The pooled product was size selected on a 2% E-gel (Life Technologies, Waltham, MA), then recovered based on expected fragment size with a Qiagen (Hilden, Germany) gel extraction kit. Cleaned, size-selected products were run on an Agilent Bioanalyzer to confirm the expected profile and determine the average product size.

The size-selected pool was qPCR quantitated and loaded onto one MiSeq flowcell using a MiSeq 600-cycle sequencing kit, version 3 for 300 bp paired-end sequencing using a MiSeq FGx system in RUO mode. After sequencing, read data was translated into FASTQ files using the Illumina bcl2fastq 1.8.4 software with an ASCII offset of 33. PhiX DNA reads (used as a spike-in control) were removed by alignment to the PhiX genome. The Roy J. Carver Biotechnology Center used in-house scripts for sorting the reads (with two mismatches allowed in the 5' primer sequences) and demultiplexing (with one mismatch allowed in the index sequence attached in library prep).

Sequence Analyses

UPARSE (Edgar, 2013) was used to analyze the amplicon sequence data. Primers from forward and reverse reads were sorted and demultiplexed. The paired-ends were joined and quality filtered at Phred quality score of 20. The last 20 bp were removed from both ends. Sequences with minimum merge length < 80 bp were discarded. Sequencing reads were clustered into operational taxonomic units (OTUs) at 97% nucleotide sequence identity. Representative sequences from each OTU were compared to the NCBI database using BLAST to ensure sequence specificity and only *nirK* and *nirS* sequences were retained for further analyses.

Diversity analyses were conducted using QIIME (Quantitative Insights into Microbial Ecology) (Caporaso et al., 2010). Rarefaction was performed at multiple depths between one and the rarified depth (set to the median number of sequences for each gene). For *nirK*, samples containing fewer than 13,000 total sequences were excluded from analysis based on rarefaction curves (Figure S1). For *nirS*, samples containing fewer than 1,000 total sequences were excluded from analysis based on rarefaction curves (Figure S1). The number of observed OTUs and Chao1 richness estimates for each gene were determined using alpha diversity analyses in QIIME.

Phylogenetic Analyses

Representative nucleotide sequences of the observed OTUs were aligned in Geneious v8.1.8 (Kearse *et al.*, 2012) using the FFT-NS-2 algorithm within MAFFT v7.017 (Katoh et al., 2002) and manually checked and trimmed. The alignment length for *nirK* was 123 bp and *nirS* was 417 bp. Maximum likelihood trees were constructed for representative sequences of observed OTUs using FastTree v2.1.5 package (Price *et al.*, 2010) in Geneious v8.1.8, with Jukes-Cantor Correction and 1,000 resamples without branch length reoptimization. Trees were visualized using the Interactive Tree of Life (iTOL) (Letunic and Bork, 2016). The normalized average relative

abundance was plotted for each OTU: OTU relative abundance averaged by region, then divided by the sum of the averages for all regions.

Statistical Analyses

Hierarchical Clustering (HCL) was performed on normalized physicochemical parameters (with each parameter summing to one in order to compare scale across variable units) and on the relative abundance values for each OTU within each sample site. The clustering method used a centered Pearson correlation distance matrix and average linkage clustering (using Multi-experiment Viewer, MeV 4.8; www.tm4.org/mev/) (Saeed et al., 2003). For clustering analysis only, 0.000001 was added to counts of zero to avoid software adjustments of zero values. HCL for chemistry only included parameters measured in at least 50% of the samples.

Correlations between community composition and environmental parameters were analyzed by canonical correspondence analysis (CCA) using the program Canoco, version 5 (Ter Braak, 1985). CCA was used to determine if the denitrifier community structure was more strongly correlated to specific environmental variables than expected by chance. Relative abundance of sequences for each OTU (defined at 97%) was used as the species input and environmental parameters were used as possible explanatory variables. Environmental parameters were included in the analysis if they were measured (above detection limits) in 15 or more samples. All dissolved metals (DM) were excluded from the analysis as these values were covarying with total recoverable metals (TRW). For *nirK* and *nirS*, environmental parameters from surface sediments included in the analyses were: pH, temperature (˚C), conductivity (µS/cm) and dissolved oxygen (mg/L). For *nirK*, total recoverable metals (TRW in surface water; µg/L) included in the CCA analyses were Ca, Fe, Mg, Mn, Na, Sr, and Zn. For *nirS*, total recoverable metals (TRW in surface water; µg/L) included in the CCA analyses were Al, Ca, Cu, Fe, Pb, Mg, Mn, Na, Sr, and Zn.

Significant environmental parameters (p-values < 0.05) after Bonferroni correction were selected via forward selection and included in analysis.

Spearman correlations between environmental parameters and the relative abundance of individual OTUs were performed in QIIME (observation_metadata_correlation.py) with Bonferroni corrected p-values < 0.05. Environmental parameters included in the analysis were the same as those used for CCA, with the addition of dissolved metals (DM in surface water; μg/L): Ca, Mg, Mn, Na, Sr, and Zn for *nirK*; Fe, Mg, Mn, Na, Sr, and Zn for *nirS*.

CHAPTER 4

RESULTS

Environmental Parameters

The sampling area was divided into four separate regions (Caribbeau, New Dominion, Iron Bog, and Howard Fork) based on chemistry and mining history (Figure 2). Sites within Caribbeau and New Dominion were actively mined for approximately 75 years and still emit visible AMD today. The CSIB site was an EPA-remediated site that was receiving AMD from a different source than the other New Dominion sites and had unique environmental characteristics. Sites within Iron Bog are receiving acid rock drainage, a chemical equivalent to AMD, generated through natural groundwater. The Howard Fork samples were taken directly from the Howard Fork river (upstream of the other AMD regions). This site is not located near a mine but likely receives intermittent AMD runoff from small mines further up the drainage basin.

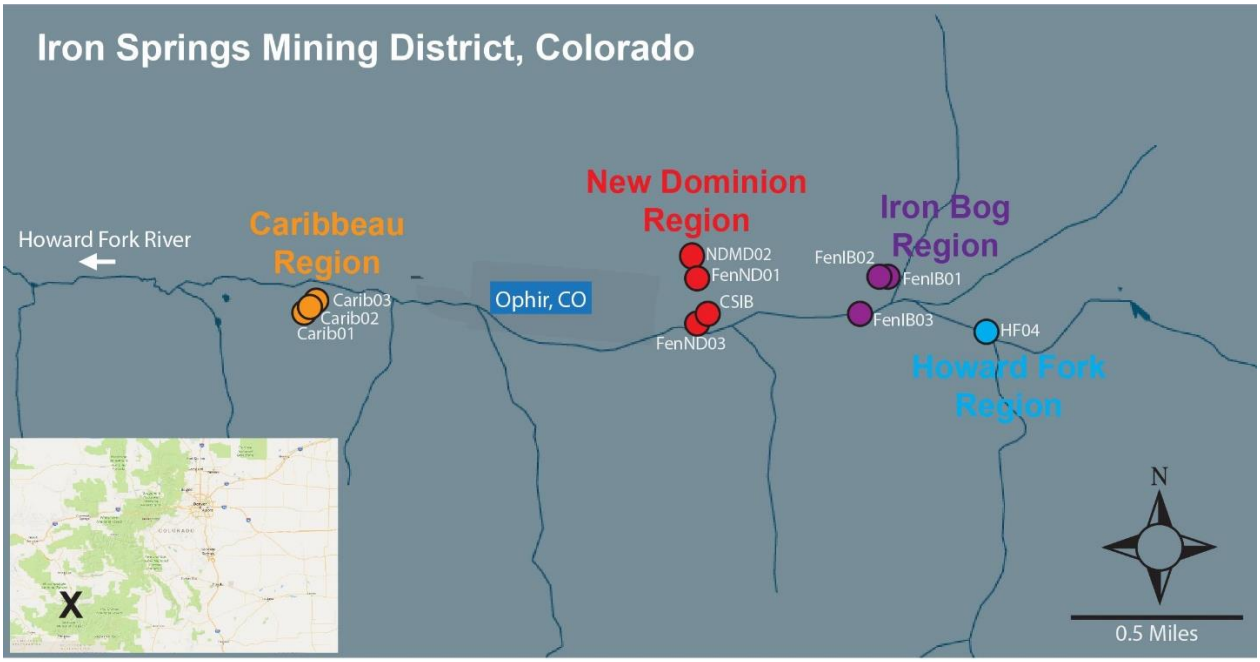

Figure 2. Map of sampling regions and individual sites within the Iron Springs Mining District located in Southwest Colorado. Base image modified from Google Maps (https://www.google.com/maps/).

Each region contains its own, unique physical and chemical characteristics, which is likely a repercussion of the complex geology within the Iron Springs Mining District that varies among the four regions. Across all individual samples, pH ranged from 3.2-8.3, temperature ranged from 6.6˚C-22.4˚C, dissolved oxygen levels ranged from 1.0-10.0 mg/L, and conductivity ranged from 296-1608 μS/cm. Sediment pH averaged 7.3 within Caribbeau, 5.5 within New Dominion, 4.8 within Iron Bog, and 7.0 for Howard Fork. The pH within New Dominion varied across sites and time points (pH 3.2-8.1). Temperature averaged 8.4˚C at Caribbeau, 13.3˚C at New Dominion, 13.7˚C at Iron Bog, and 9.9˚C at Howard Fork. Dissolved oxygen was highest at Caribbeau (average of 8.4 mg/L) and lowest at Iron Bog (average of 5.12 mg/L). Conductivity was highest at New Dominion (average of 1238.4 μS/cm) and lowest at Howard Fork (315.5 μS/cm). A comparison of the sum of dissolved metals to conductivity at each site resulted in a Pearson correlation coefficient of 0.83 and an R^2 value of 0.68 (Figure S5). The most abundant metals in the surface water (total recoverable metals) were aluminum, iron, manganese, and zinc (>10 mg/L). Strontium, barium, copper, cadmium, lead, and nickel were found in lower amounts. Other metals commonly found in AMD, such as arsenic, were below detectable limits at most sites and time points. Hierarchical clustering (HCL) of chemistry data revealed clusters according to sampling regions and sites within, indicating that each region, as a whole, has distinct chemical characteristics (Figure 3).

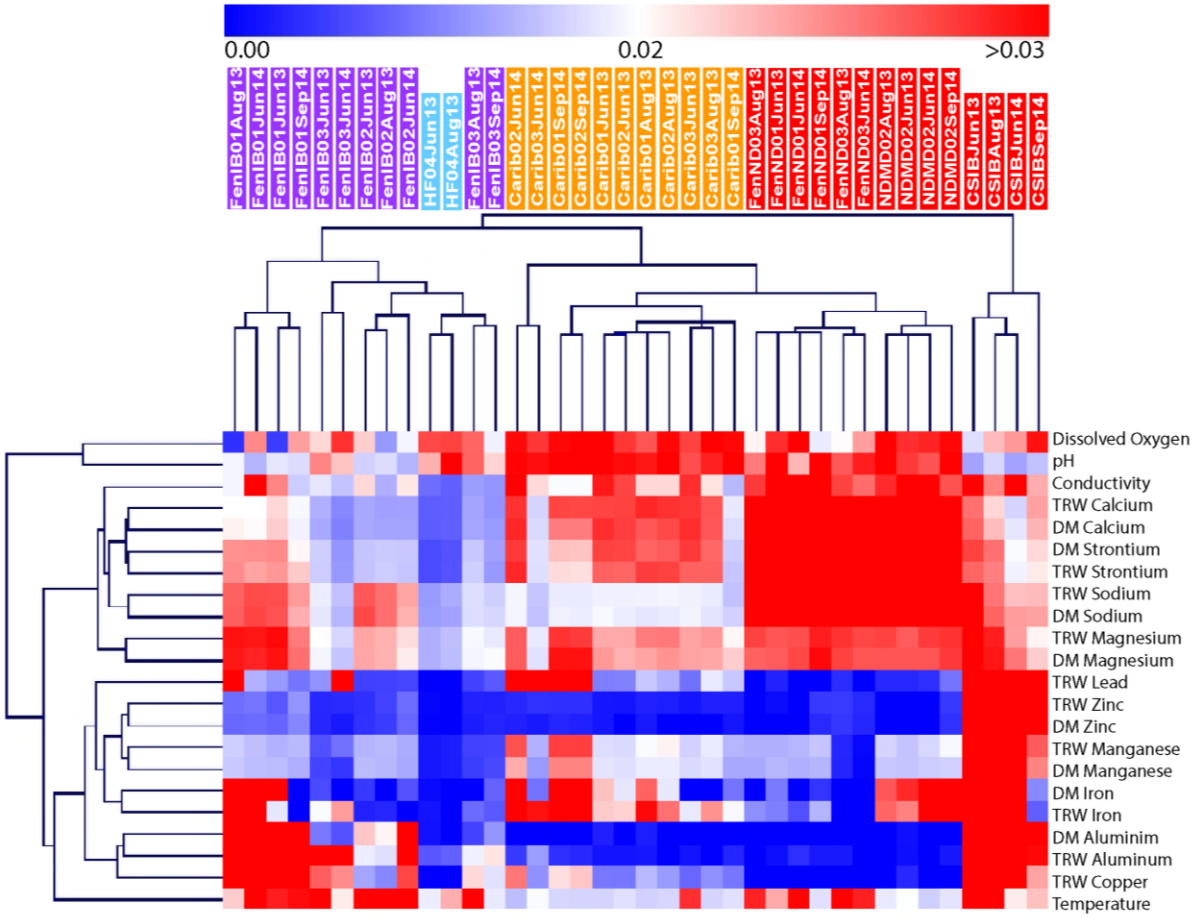

Figure 3. Hierarchical clustering map of environmental chemistry data using analytes present in at least 50% of samples. Analyte values were normalized to a sum of 1. Scale bar indicates the proportion of the normalized sum. Chemistry data clusters according to sampling region, as indicated by colored labels.

Table 3.1: Chemistry data from surface water for sample sites across June and September 2013 in the Iron Springs Mining District

Sample Region	Sample Name	Sample Date	pH	Cond. (µS/cm)	Temp. (°C)	DO (mg/L)
Caribbeau Mine	Carib01Jun13	6.25.13	7.3	1095	7.9	8.8
Caribbeau Mine	Carib01Aug13	8.06.13	7.1	829	7.8	7.7
Caribbeau Mine	Carib02Jun13	6.25.13	7.2	1034	8.4	8
Caribbeau Mine	Carib02Aug13	8.06.13	7.8	830	8	8.5
Caribbeau Mine	Carib03Jun13	6.25.13	6.6	1068	13.1	7.9
Caribbeau Mine	Carib03Aug13	8.06.13	7	814	7.9	10
Iron Bog/Fen	FenIB01Jun13	6.25.13	4.5	945	13.4	1.4
Iron Bog/Fen	FenIB01Aug13	8.05.13	4.8	745	10.4	1.1
Iron Bog/Fen	FenIB02Jun13	6.25.13	4.1	827	18.5	6.4
Iron Bog/Fen	FenIB02Aug13	8.05.13	4.3	533	19.8	3.5
Iron Bog/Fen	FenIB03Jun13	6.25.13	6.1	700	17.4	6.3
Iron Bog/Fen	FenIB03Aug13	8.05.13	6.4	479	14.6	7.5
New Dominion Mine	FenND01Jun13	6.25.13	7.3	1380	11	8.1
New Dominion Mine	FenND01Aug13	8.05.13	6.2	1051	13.3	6
New Dominion Mine	FenND03Aug13	8.05.13	6.5	1040	18.7	5.9
New Dominion Mine	NDMD02Jun13	6.25.13	6.8	1424	9.5	8.1
New Dominion Mine	NDMD02Aug13	8.06.13	7.4	1072	8.7	8.9
New Dominion Mine	CSIBJun13	6.25.13	3.2	1529	14.9	5.1
New Dominion Mine	CSIBAug13	8.05.13	4.2	947	21.2	6.6
Howard Fork River	HF04Jun13	6.25.13	5.7	335	8.9	7.8
Howard Fork River	HF04Aug13	8.05.13	8.3	296	10.9	7.9

Table 3.2: Chemistry data from surface water for sample sites across June and September 2014 in the Iron Springs Mining District

Sample Region	Sample Name	Sample Date	pH	Cond. (µS/cm)	Temp. (°C)	DO (mg/L)
Caribbeau Mine	Carib01Sept14	9.30.2014	7.3	765	8	8.5
Caribbeau Mine	Carib02June14	6.24.2014	7.3	1230	7.1	8.5
Caribbeau Mine	Carib02Sept14	9.30.2014	7.8	763	7.9	8.7
Caribbeau Mine	Carib03June14	6.24.2014	7.2	828.3	9.3	8.0
Caribbeau Mine	Carib03Sept14	9.30.2014	8.0	562	8.4	8.5
Iron Bog/Fen	FenIB01June14	6.24.2014	3.5	1149	13.9	7.1
Iron Bog/Fen	FenIB01Sept14	9.30.2014	4.3	616	13.7	6.9
Iron Bog/Fen	FenIB02June14	6.24.2014	3.5	808.1	15.3	5.7
Iron Bog/Fen	FenIB03June14	6.24.2014	5.5	591.8	9.9	8.1
Iron Bog/Fen	FenIB03Sept14	9.30.2014	5.4	450	8.7	5.5
New Dominion Mine	FenND01June14	6.24.2014	5.7	1608	13.9	9.2
New Dominion Mine	FenND01Sept14	9.30.2014	7.3	1575	8.4	5.4
New Dominion Mine	FenND03June14	6.24.2014	7.0	980	13.3	6.9
New Dominion Mine	NDMD02June14	6.24.2014	6.5	1602	7.7	8.2
New Dominion Mine	NDMD02Sept14	9.30.2014	8.1	1017	8.5	8.5
New Dominion Mine	CSIBJune14	6.24.2014	3.2	1242	9.9	7.0
New Dominion Mine	CSIBSept14	9.30.2014	3.8	890	10.6	8.4

Community Composition and Phylogeny of *nirK* Gene Sequences

nirK gene sequences were recovered from 9 out of 11 different sample sites spanning all four regions (25 individual samples in total). Amplicon sequencing resulted in a total of 940,279 paired-end reads for *nirK* across all samples, with 13,291 to 90,423 *nirK* reads per sample. From all sites combined, we recovered a total of 253 unique *nirK* OTUs defined at a 97% identity cut-off. Between 7-51 *nirK* OTUs were observed in each individual sample (Figure S2). Samples from the Caribbeau region contained the highest number of OTUs (30-51 OTUs), whereas the lowest number of OTUs was observed in the Iron Bog samples (7-22 OTUs). Chao1 richness estimates ranged from 13-74 OTUs for each sample (Figure S2). The difference between the number of observed OTUs and the estimated total number of OTUs (Chao1 estimate) ranged from 0-10 across all sites except sites Carib02Sep14, Carib03Jun13, and Carib03Jun14, and Carib02Aug13 that had a difference of 10.5-28. This indicates that the majority of the *nirK* genes were sequenced in each sample (with the exception of the four Caribbeau sites).

Phylogenetic analysis of *nirK* OTUs revealed large evolutionary distance among sequences from sites in close proximity within the Iron Springs Mining District (Figure 4). Thirteen OTUs from the Caribbeau region were phylogenetically similar to each other and clustered according to sampling region. Otherwise, most OTUs from the same region were phylogenetically disparate. For instance, OTUs predominantly found at Howard Fork (blue) or Iron Bog (purple) were distributed across the tree without site- or region-specific clustering. Phylogenetically similar OTUs were found at sites with very different chemistry (e.g., nirK_OTU_78 and nirK_OTU_408 with 89%ID were found at Howard Fork and Iron Bog with drastically different iron concentrations of 381 and 5960 μg/L, respectively).

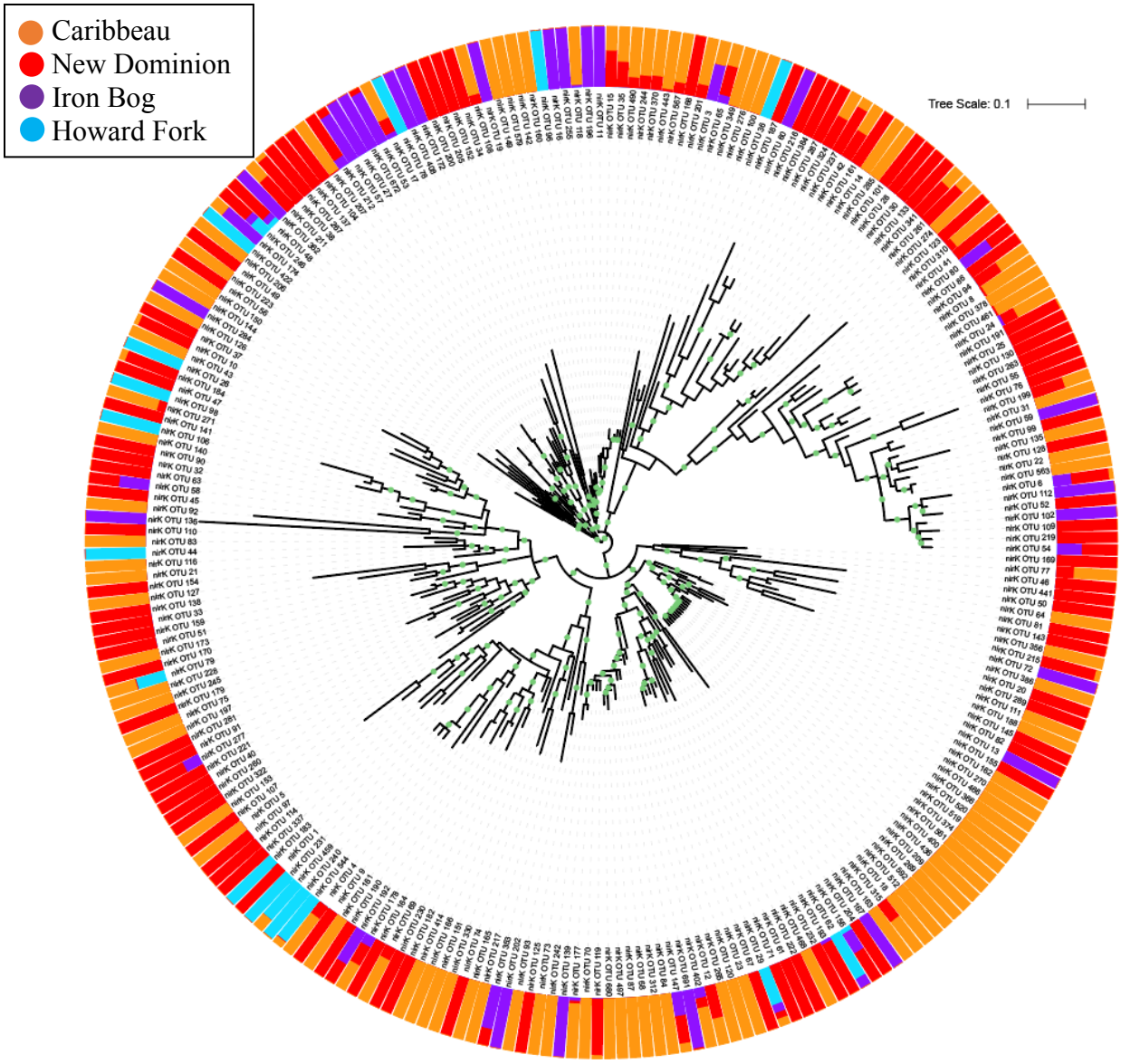

Figure 4. Maximum likelihood tree for nirK gene sequences across all regions within the Iron Springs Mining District using FastTree v2.1.5 package (Price et al., 2010) in Geneious v8.1.8, with Jukes-Cantor Correction and 1,000 resamples without branch length reoptimization. Bootstrap values above 75.0% indicated by green circle. The relative abundance of OTUs across regions (as indicated by colored bars) shows large evolutionary distance among sequences within close proximity**.**

Iron Springs *nirK* sequences were related (76%-100% nucleotide identity) to *nirK* sequences from other environments, including agricultural soils, freshwater environments, and soils impacted by heavy metals (based on BLAST searches to the NCBI database). nirK_OTU_255 was identical to an OTU found in agricultural plots in Japan (NCBI accession DQ783709). nirK_OTU_231 was identical to an OTU found within an oligotrophic, alpine lake microbial mat in the Central Pyrenees, Spain (NCBI accession KF816401). Thirteen OTUs found within the Caribbeau and New Dominion regions were closely related (>90% nucleotide identity) to silver-tolerant OTUs from topsoil (pH of 7.8) in Alunda, Uppsala, Sweden (Throbäck et al., 2007).

A majority of the *nirK* OTUs were found in one site or region: 101 OTUs (40% of all *nirK* OTUs) were found at a single site and 153 OTUs (60%) were found in just one region. Among these, 62 OTUs (24%) were only found in the Caribbeau region, 68 OTUs (27%) were only found in the New Dominion region, 15 OTUs (6%) were only found in the Iron Bog region, and 8 OTUs (3%) were only found in the Howard Fork region. Nearly 30% of the OTUs were shared between two regions: A smaller percentage of OTUs (11%; 29 OTUs) were found in three different regions. Caribbeau and New Dominion regions shared the most OTUs (75), while Iron Bog and Howard Fork shared the fewest (5). Only one OTU was found in all four regions: nirK_OTU_29, which had a nearest BLAST hit (88% identity) to a sequence found in agricultural soil.

Hierarchical clustering (HCL) analysis of the relative abundance of each *nirK* OTU across samples revealed that the Howard Fork, Iron Bog, and Caribbeau Mine samples clustered independently from each other (Figure 5). The New Dominion samples clustered closely with Iron Bog and Caribbeau Mine samples. HCL clustering revealed 16 distinct groups of *nirK* OTUs that had significant changes in the relative abundance between sites/regions, defined as OTUs with an average relative abundance at least four times higher than the average relative abundance across

all sites. A majority of the groups were specific to one region: four Caribbeau Mine groups comprised of 67 total OTUs; one Iron Bog group comprised of three OTUs; seven New Dominion groups comprised of 62 total OTUs; and one Howard Fork group comprised of 24 OTUs. Groups 14-16 represent OTUs that were found in two regions (Iron Bog and New Dominion or Caribbeau Mine and New Dominion). OTUs within each group displayed great sequence diversity with low percent identities (75% on average) and high phylogenetic distances.

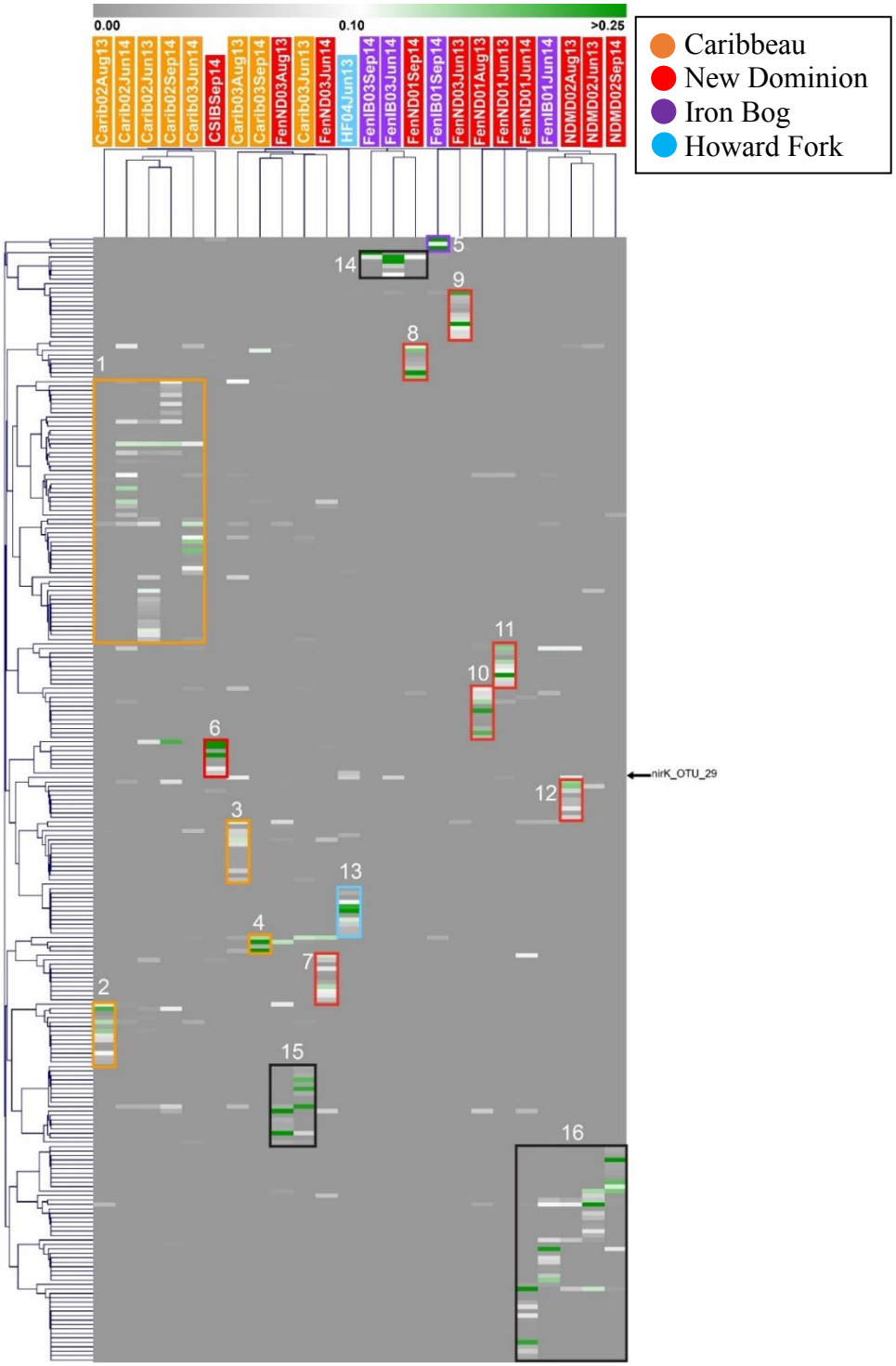

Figure 5. *nirK* hierarchical clustering map using Pearson correlation of relative abundance of individual OTUs. Scale bar represents relative abundance from 0.00 to greater than 0.25. OTU groups (in boxes color coded by region) were defined as those where the average relative abundance of OTUs within each group was at least four times the average relative abundance across all sites. Groups color coded black contained OTUs present across multiple regions. nirK_OTU_29 (present across all regions) indicated by arrow.

Community Composition and Phylogeny of *nirS* Gene Sequences

nirS sequences were recovered from all four regions and all 11 sample sites, totaling 26 individual samples. Amplicon sequencing resulted in a total of 277,979 paired-end reads for *nirS* across all samples. The number of *nirS* reads per sample ranged from 1,033 to 59,838. From all sites combined, we recovered a total of 260 unique *nirS* OTUs defined at a 97% identity cut-off. Both the lowest and highest number of OTUs was observed in the Caribbeau region (5-80 OTUs) and Chao1 richness estimates ranged from 5-87 OTUs for each sample (Figure S2). The difference between the number of observed OTUs and the estimated total number of OTUs (Chao1 estimate) ranged from 0-7, indicating that the majority of *nirS* genes were sequenced in each sample.

Similar to *nirK*, phylogenetic analysis of *nirS* sequences within the Iron Springs Mining District revealed large evolutionary distance among sequences from sites in close proximity (Figure 6). Sequences that were similar in their distribution across the study area were phylogenetically disparate. For example, Howard Fork, which contained the highest percentage of endemic species, showed little phylogenetic clustering. Phylogenetically similar OTUs were found at sites with very different chemistry (e.g., nirS_OTU_104 and nirS_OTU_373 with 92% similarity found at Howard Fork and Caribbeau sites with very different iron concentrations; 381 and 4930 μg/L, respectively).

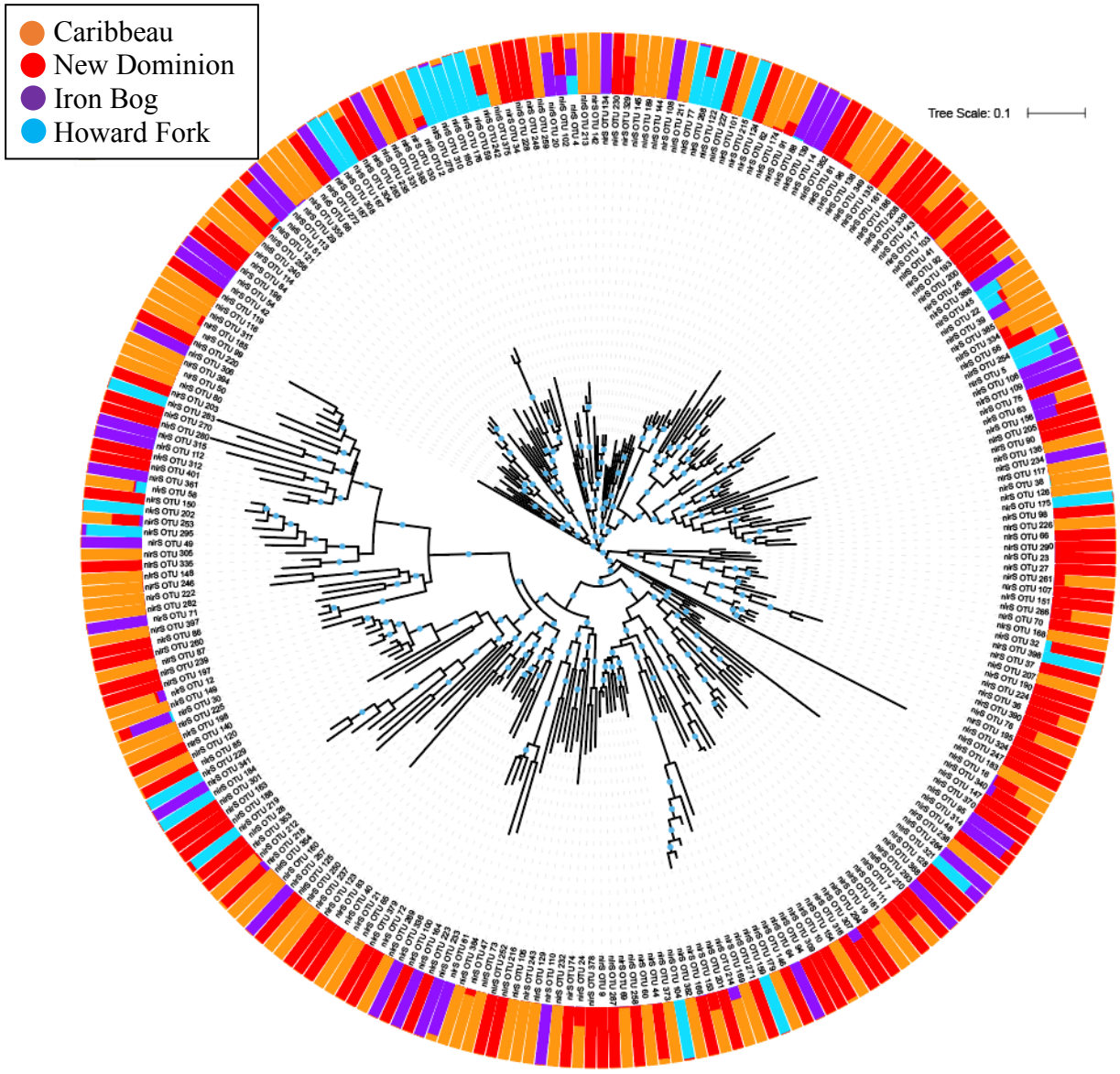

Figure 6. Maximum likelihood tree for *nirS* gene sequences across all regions within the Iron Springs Mining District using FastTree v2.1.5 package (Price *et al.*, 2010) in Geneious v8.1.8, with Jukes-Cantor Correction and 1,000 resamples without branch length reoptimization. Bootstrap values above 75.0% indicated by blue circle. The relative abundance of OTUs across regions (as indicated by colored bars) shows large evolutionary distance among sequences within close proximity.

Iron Springs *nirS* sequences were related (78%-100% identity) to *nirS* sequences from other environments, including agricultural soils, fen soils, and freshwater environments (based on BLAST searches to the NCBI database) nirS_OTU_95 was closely related (98% identity) to an OTU found within pH-neutral fen soils in Denmark (Palmer and Horn, 2015). nirS_OTU_205 was closely related (90% identity) to an OTU found in mercury-contaminated soil (NCBI accession JF261040). The Howard Fork region contained 13 OTUs that were closely related (>85% identity) to OTUs found in freshwater environments (NCBI accession AM419565, JN179246, GU393102, KT444058, GU322137, DQ337856, GU393043, AM419582, HG800325, AB937597, EF615473, JF966853, AM419564).

A majority of the *nirS* OTUs were found at a single site (111 OTUs; 43% of all *nirS* OTUs) or in a single region (166 OTUs; 64%). Among those, 62 OTUs (24%) were only found in Caribbeau, 68 (26%) were only found in New Dominion, 24 (9%) were only found in Iron Bog, and 10 (4%) were only found in Howard Fork. Approximately one-third of the OTUs were shared among more than one region, with Caribbeau and New Dominion sharing the most OTUs (59) and Howard Fork/Caribbeau and Howard Fork/New Dominion sharing the fewest OTUs (13). Five OTUs were found across all four regions (nirS_OTU_4, nirS_OTU_5, nirS_OTU_58, nirS_OTU_30, nirS_OTU_45). These five OTUs were genetically dissimilar from each other (68.6% average identity), but were similar (85-97% identity) to database sequences from freshwater river sediment (nirS_OTU_4), agricultural soil (nirS_OTU_5 and nirS_OTU_45), glacier foreland soil (nirS_OTU_58), and the biofilm of a freshwater lake (nirS_OTU_30). nirS_OTU_2 was found at 3 regions and made up >10% of sequences at nine individual sites, including 94% at Carib01Aug13 and 75% at Carib01Jun13.

Hierarchical clustering (HCL) analysis of the relative abundance of each *nirS* OTU across samples revealed that the most of the Caribbeau Mine samples clustered independently from each

other (Figure 7). Four of the New Dominion samples clustered independently from all other samples. Howard Fork samples clustered together, but also with an Iron Bog sample. HCL clustering revealed 10 distinct groups of *nirS* OTUs that had significant changes in the relative abundance between sites/regions (defined as OTUs with an average relative abundance at least 10 times higher than the average relative abundance across all sites). All of the groups were specific to one region: one Caribbeau group comprised of six OTUs; five New Dominion groups comprised of 74 total OTUs; two Iron Bog groups comprised of 104 total OTUs; two Howard Fork groups comprised of 22 total OTUs. OTUs within each group displayed great sequence diversity with low percent identities (70% on average) and high phylogenetic distances.

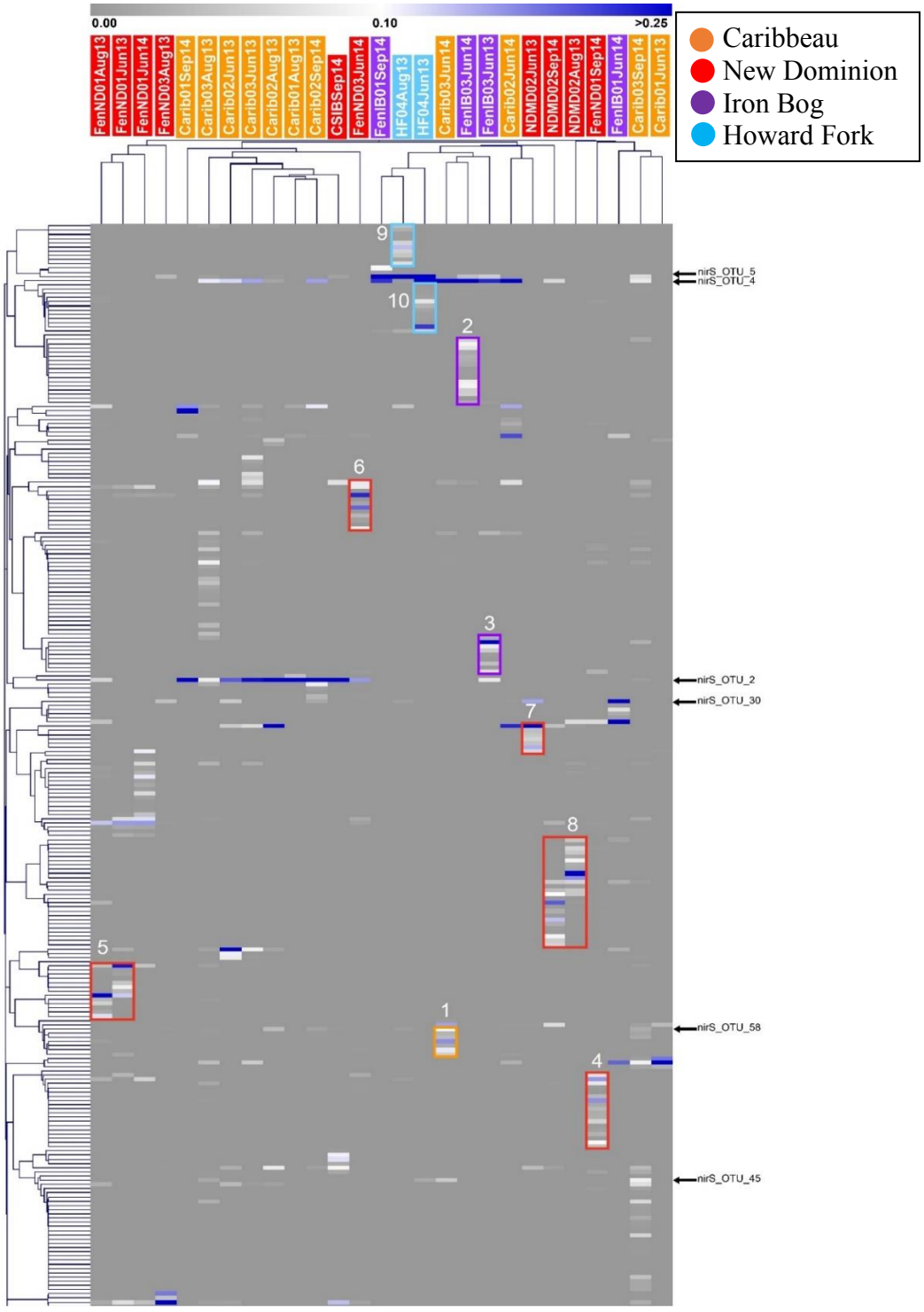

Figure 7. nirS hierarchical clustering map using Pearson correlation of relative abundance of individual OTUs. Scale bar represents relative abundance from 0.00 to greater than 0.25. OTU groups (in boxes color coded by region) were defined as those where the average relative abundance of OTUs within each group was at least ten times the average relative abundance across all sites. OTUs spread across all regions and OTU of interest nirS_OTU_2 are indicated by arrows**.**

Relationship Between Environmental Parameters and Gene Sequences

Sediment pH was not correlated to *nirK* or *nirS* richness, overall community structure, or relative abundance of individual OTUs. There was a slightly positive trend between the number of observed *nirK* OTUs and pH, though the relationship was not significant (R^2=0.26; Figure S3). There was no trend observed between the number of observed *nirS* OTUs and sediment pH (R^2=0.04; Figure S3). Spearman rank correlations did not show a significant relationship between pH and the relative abundance of individual *nirK* or *nirS* OTUs. Canonical correspondence analysis (CCA) did not reveal a significant relationship between pH and the overall *nirK* or *nirS* community structure.

Spearman correlations revealed that the relative abundance of nirK_OTU_14 was significantly negatively correlated to temperature (rho = -0.71) and nirS_OTU_2 was significantly positively correlated to dissolved manganese (rho = 0.86) and total recoverable copper (rho=0.87).

CCA showed the *nirK* community was correlated to DM Strontium (Figure 8) and showed that the *nirS* community was correlated to conductivity, total recoverable calcium, total recoverable iron, and total recoverable sodium (Figure 9). When the *nirS* relative abundance HCL groups (Figure 7) were highlighted on the CCA diagram, it suggested that the OTUs that formed HCL groups were driving much of the overall community structure (Figure 9). For instance, the Howard Fork HCL groups 9 and 10 were distinctly clustered on the CCA plot, based in part on the low conductivity and iron values at those sites. The New Dominion HCL groups all had relatively high conductivity values (>980 μS/cm), but were separated by iron levels. When analyzing individual regions on their own, the New Dominion *nirS* OTUs were significantly correlated to total recoverable iron (Figure S4), further suggesting that these sites were driving the relationship with iron seen in the analysis of the overall community structure (Figure 9).

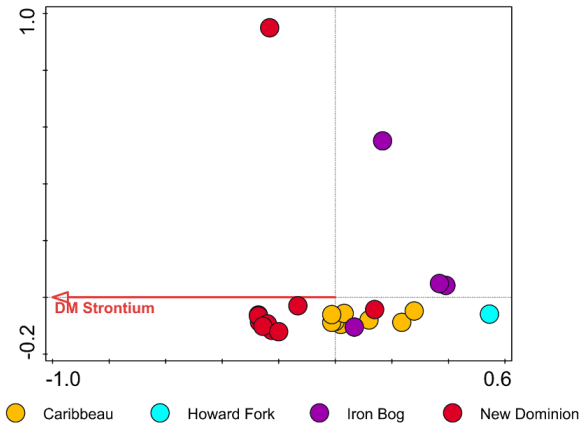

Figure 8. Canonical Correspondence Analysis (CCA) of relative gene abundance of *nirK* gene sequences. DM (dissolved metal) strontium significantly (Bonferroni corrected p-value <0.05) correlated to *nirK* distribution across the Iron Springs Mining District.

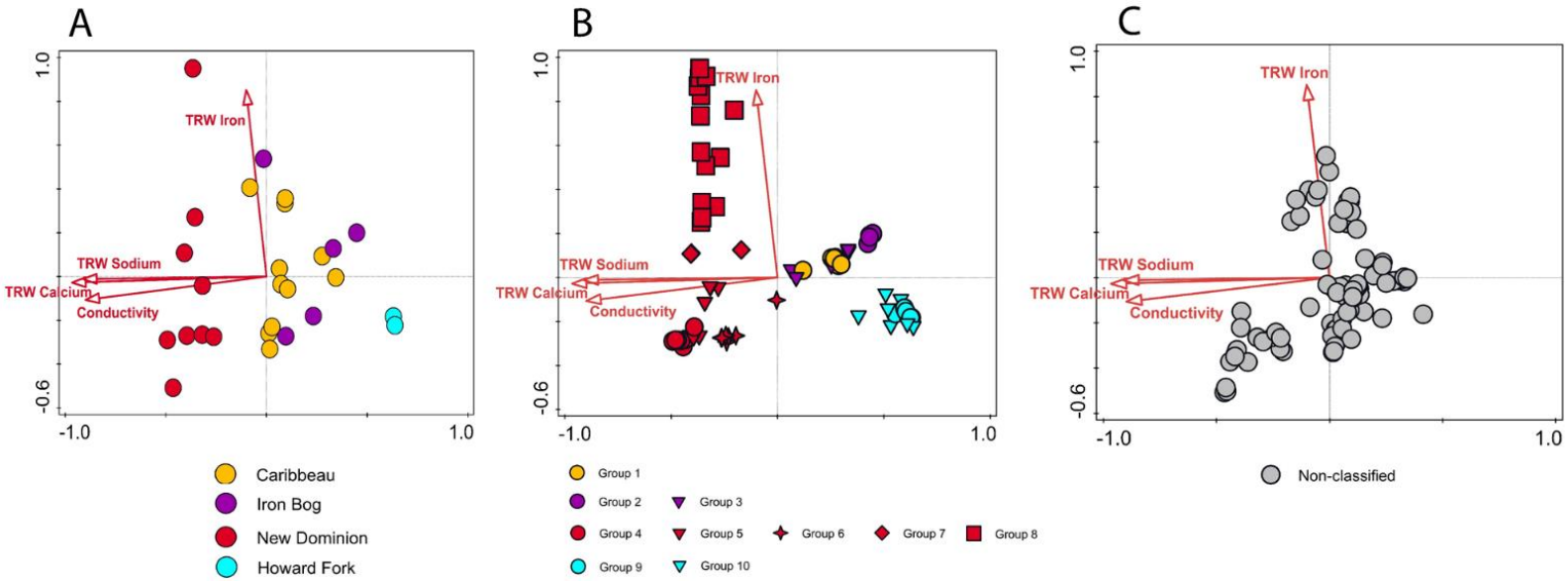

Figure 9. Canonical Correspondence Analysis (CCA) of relative gene abundance of *nirS* gene sequences (Panel A). Conductivity, TRW (total recoverable metals from surface water) Iron, TRW Sodium, and TRW Calcium significantly (Bonferroni corrected p-value <0.05) correlated to *nirS* distribution across the Iron Springs Mining District. Samples within each region are indicated by a colored circle. Panel B contains OTUs found within individual HCL groups as shown in Figure 7. Panel C contains all OTUs that were not found within individual HCL groups shown in Figure 7.

Seasonal Variations in Gene Sequences

Within both sampling years, 46% of *nirK* OTUs and 45% of *nirS* OTUs were present. Within multiple sampling months, 50% of *nirK* OTUs and 49% of *nirS* OTUs were present. Pearson and Spearman correlations did not reveal a significant relationship between seasonality and the number of observed OTUs at each site for either *nirK* or *nirS*. Changes in the relative abundance of individual OTUs across sites does not appear to be linked to seasonality as relative abundance-based hierarchical clustering did not reveal nodes segregated by sampling month (e.g., Caribbeau samples taken in June, August, and September all clustered together for both *nirK* and *nirS*). CCA did not show a significant relationship between sampling month and the relative abundance of gene sequences for either group.

CHAPTER 5

DISCUSSION

AMD is a widespread environmental hazard that can severely damage aquatic ecosystems. Little is known about how *nirK* and *nirS* gene sequences are distributed within an AMD environment. In this study, we determined the diversity, phylogeny, and distribution of *nirK* and *nirS* gene sequences within four distinct regions in AMD-impacted sediments at the Iron Springs Mining District in Southwestern Colorado. Although gene sequences are not a proxy for function, analyses of the separate gene groups suggest that each have the potential for denitrification as a high number of OTUs (253 for *nirK* and 260 for *nirS*) were observed across the entire sampling area with varying relative abundance patterns. The presence of 117 *nirK* and 116 *nirS* OTUs shared across two sampling years may suggest that many of the *nir* OTUs permanently reside in the sediments, and are not merely washed in from the surrounding watershed.

Hierarchical clustering revealed that the relative abundance patterns of *nirK* and *nirS* OTUs were often similar among sites within a sampling region but more dissimilar between regions (e.g., most Caribbeau samples clustered together on the *nirK* and *nirS* HCL plots, separate from other regions). Previous studies also found similar patterns of site/region specificity for *nirK* and *nirS* (Santoro et al., 2006; Smith and Ogram, 2008; Mosier and Francis, 2010). One *nirK* OTU and five *nirS* OTUs displayed a cosmopolitan distribution across all four sampling regions, which may represent either *nirK/nirS*-containing organisms tolerant of a range of pH and metal conditions or organisms that have been transported between sites by dispersion.

Previous work has shown pH to be an important factor in controlling denitrifying communities in the environment. Diversity and productivity generally decreases with acidic pH (Baesman et al., 2006; Wallenstein et al., 2006; Saleh-Lakha, 2009). Evidence has shown the

optimum pH range for complete reduction of nitrate to nitrogen gas is pH 6-8, below which the proportion of intermediate products (nitric and nitrous oxides) increases (Knowles, 1982; Nägele and Conrad, 1990). However, some studies have shown denitrification to occur and even thrive at an acidic pH. The optimum pH for denitrification rates in historically acidic soils was 3.90 (Parkin et al., 1985). Denitrification rates were >99% of the optimum at a pH of 5.3-5.75 within synthetic wastewater (Di Capua et al., 2017). These results indicate that denitrifier communities are able to metabolize in acidic conditions, perhaps especially if they are found within a historically acidic environment and have been able to adapt. In Iron Springs, pH ranged from 3.2-8.3 across all sample sites, but did not correlate to the number of observed *nir* OTUs, the relative abundance of any specific *nir* OTU, or the overall community structure or phylogeny of either gene group. Although there is a general increase in the number of observed *nirK* OTUs as pH increases, substantial variation exists around this trend. Because a decrease in pH will increase metal solubility, it is likely that changes in pH have indirect effects on the denitrifier community. These results may indicate that the community is well adapted to a low pH environment, but incubation studies are needed to determine whether or not denitrification rates at these sites is impacted by pH.

Denitrification enzymes are located on or near the outer cell surfaces, which makes them especially vulnerable to chemical disruption. Metals have been shown to affect denitrifier diversity and inhibit denitrification in a way that differentially affects the steps in the reduction of nitrate to nitrogen gas, with nitrite reductase being the most sensitive step within the denitrification pathway (Bollag and Barabsz, 1979; Sakadevan, et al., 1999; Sobolev and Begonia, 2008, Liu et al., 2016). However, other studies have shown diversity to increase with the addition of specific metals (Throbäck et al., 2007; Sandaa et al., 2001). In the present study, metal concentrations (e.g., Al, Cu, Fe, and Zn) in the Iron Springs region exceed the allowable concentrations as determined by the Colorado Department of Public Health and Environment (CDPHE) Regulation 3;

concentrations that have been shown to harm terrestrial and aquatic life (Colorado Water Quality Control Commission, 2012). Nonetheless, *nirK* and *nirS* OTUs were observed at sites with very high metal concentrations (>10 mg/L), which may indicate that these organisms are tolerant of these harsh conditions. Iron, in particular, appeared to play a role in shaping the *nirS* community structure (based on CCA results; Figure 9). Rates of denitrification in an AMD environment have been shown to substantially decrease with the addition of ferric or ferrous iron above background, likely due to chemical disruption of the cell wall (Baesman et al., 2007). Iron can also strongly complex with organic matter and reduce the bioavailability of organic carbon to denitrifiers (McKnight and Bencala, 1990). Iron concentrations differentially affected *nirS* communities within the New Dominion region, indicating potential adaptability to high iron concentrations in some OTUs (Figure S4).

The total *nirS* community composition was strongly correlated to conductivity or conductivity-related ions (calcium and sodium; based on CCA analysis; Figure 9). Conductivity may be an indication of the total dissolved metal concentration (Figure S5). Dissolved metals are those that are bioavailable and thus more likely to have toxic effects on microbes. The denitrifying microbes within Iron Springs may be resistant to dissolved metals as a result of long term genetic modification, spread of resistance genes, or the replacement of metal-sensitive strains by strains more tolerant of dissolved metals (Holtan-Hartwig et al., 2002). Interestingly, prior work with these same samples showed that organisms involved in nitrification may have also been influenced by conductivity (overall community structure and relative abundance of individual OTUs were correlated to conductivity) (Ramanathan, 2016). Overall, these findings may implicate conductivity, and possibly dissolved metal concentrations, as a driving factor in controlling nitrogen cycling in these sediments.

Other organisms not studied here may also contribute to denitrification in the Iron Springs region. For instance, other *nirK* and *nirS* gene sequences that were not detected with the conventional primer sets used here may be present (Wei et al., 2015). Additionally, fungal denitrifiers have the potential to convert nitrate to nitrogen gas within acidic environments. Fungal denitrification has occurred in groundwater with a pH of 3.67 (Jasrotia et al., 2014). Certain species have shown evidence of denitrification in an AMD environment (at pH 1) and express transcripts for aerobic respiration and denitrification in order to adapt to fluctuating conditions (Mosier et al., 2016). The possibility for other denitrifiers that may contribute to nitrogen cycling in the Iron Springs region warrants further inquiry.

Understanding how denitrification functional genes relate to the harsh conditions of an AMD environment shows how this widespread pollutant may broadly affect the nitrogen cycle. This understanding may also allow us to better utilize the ecosystem services provided by denitrifiers: the conversion of nitrate to nitrogen gas and improvement of water quality. Nitrogen pollution can cause a suite of problems ranging from eutrophication and extensive kills of aquatic species to methemoglobinemia and birth defects in humans (Camargo and Alonso, 2006). Denitrifier services are utilized in wastewater treatment facilities around the globe that seek to reduce nitrogen pollution and some facilities have recently begun to isolate strains of denitrifiers within critically polluted environments to treat special industrial wastes (Kim et al., 2014). The denitrifiers within the Iron Springs Mining District, and perhaps other environments affected by AMD, have the potential to serve a similar purpose and treat wastewater that is acidic and contains high concentrations of metals.

Conclusions

Denitrifying microbes provide an important ecosystem service in the conversion of nitrate to nitrogen gas. Gaining a better understanding of how these microbes respond to adverse environmental conditions, like those that exist in an AMD environment, may improve our understanding of their adaptability and our own ability to utilize this service. This study has demonstrated broad community composition patterns for two denitrification functional genes, *nirK* and *nirS*, in an environment impacted by AMD. Neither gene group was significantly affected by pH, possibly indicating that these organisms are well adapted to acidic conditions. Both gene groups had high numbers of observed OTUs across all sampling sites (253 for *nirK* and 260 for *nirS*) but were differentially affected by environmental conditions. *nirK* community composition was correlated to strontium concentrations. *nirS* community composition was correlated to conductivity, sodium, calcium, and iron concentrations, which resulted in distinct groups of OTUs segregated by sampling region or individual samples. These findings improve upon our understanding of the potential for denitrification within an ecosystem impacted by AMD and provide a foundation for future research into the rates and physiology of denitrifying organisms.

REFERENCES

Altabet, M.A., Higginson, M.J., & Murray, D.W. (2002). The effect of millennial-scale changes in Arabian Sea denitrification on atmospheric CO2. *Nature* **415:** 159-162.

Baeseman, J.L., Smith, R.L., & Silverstein, J. (2006). Denitrification Potential in Stream Sediments Impacted by Acid Mine Drainage: Effects of pH, Various Electron Donors, and Iron. *Microbial Ecology* **51**: 232-241.

Baker, B.J., & Banfield, J.F. (2003). Microbial communities in acid mine drainage. *FEMS microbiology ecology* **44:** 139-152.

Bollag, J.M. & Barabasz, W. (1979). Effect of heavy metals on the denitrification process in soil. *Journal of Environmental Quality* **8:** 196-201

Camargo, J.A., & Alonso, Á. (2006). Ecological and toxicological effects of inorganic nitrogen pollution in aquatic ecosystems: a global assessment. *Environment international* **32**: 831-849.

Canfield, D.E., Alexander, N.G., & Falkowski, P.G. (2010) The Evolution and Future of Earth's Nitrogen Cycle. *Science* **330**: 192-6.

Caporaso, J. G., Kuczynski, J., Stombaugh, J., Bittinger, K., Bushman, F. D., Costello, E. K., & Huttley, G. A. (2010). QIIME allows analysis of high-throughput community sequencing data. *Nature methods* **5**: 335-336.

Cao, Y., Green, P.G., & Holden, P.A. (2008). Microbial community composition and denitrifying enzyme activities in salt marsh sediments. *Applied and environmental microbiology* 74: 7585-7595.

Colorado Geological Survey (1998) Abandoned Mine Lands. Web. http://coloradogeologicalsurvey.org/mineral-resources/abandoned-mine-lands/. Accessed 2/2/2016.

Colorado Water Quality Control Commission. (2012). Regulation No. 31 The Basic Standards and Methodologies for Surface Water.

Di Capua, F., Lakaniemi, A.M., Puhakka, J.A., Lens, P.N., & Esposito, G. (2017). High-rate thiosulfate-driven denitrification at pH lower than 5 in fluidized-bed reactor. *Chemical Engineering Journal* **310**: 282-291.

Edgar, R.C. (2013). UPARSE: highly accurate OTU sequences from microbial amplicon reads. *Nature methods* **10**: 996-998.

Einsle, O., Messerschmidt, A., Stach, P., Bourenkov, G.P., Bartunik, H.D., Huber, R., & Kroneck, P.M. (1999). Structure of cytochrome c nitrite reductase. *Nature*. **400***:* 476-480.

Fierer, N. & Jackson, R.B. (2006). The diversity and biogeography of soil bacterial communities. *Proceedings of the National Academy of Sciences of the United States of America* **103**: 626-631.

Giller, K.E., Witter, E., & Mcgrath, S.P. (1998). Toxicity of heavy metals to microorganisms and microbial processes in agricultural soils: a review. *Soil Biology and Biochemistry* **30**: 1389-1414.

Henry, S., Baudoin, E., López-Gutiérrez, J. C., Martin-Laurent, F., Brauman, A., & Philippot, L. (2004). Quantification of denitrifying bacteria in soils by nirK gene targeted real-time PCR. *Journal of Microbiological Methods* **59***:* 327-335.

Holtan-Hartwig, L., Bechmann, M., Høyås, T.R., Linjordet, R., & Bakken, L.R. (2002). Heavy metals tolerance of soil denitrifying communities: N2O dynamics. *Soil Biology and Biochemistry* **34:** 1181-1190.

Jasrotia, P., Green, S.J., Canion, A., Overholt, W.A., Prakash, O., Wafula, D., Hubbard, D., Watson, D.B., Schadt, C.W., Brooks, S.C., & Kostka, J.E. (2014). Watershed-scale fungal community characterization along a pH gradient in a subsurface environment cocontaminated with uranium and nitrate. *Applied Environmental Microbiology*. **80**: 1810–1820

Johnson, D.B., and Hallberg, K.B. (2005) Acid Mine Drainage Remediation Options: A Review. *Science of the Total Environment* **338**: 3-14.

Kandeler, F., Kampichler, C., & Horak, O. (1996). Influence of heavy metals on the functional diversity of soil microbial communities. *Biology and Fertility of Soils* **23**: 299-306.

Kandeler, E., Deiglmayr, K., Tscherko, D., & Philippot, L. (2006). Quantification of functional genes narG, nirK and nosZ of denitrifying bacteria across a glacier foreland by real time PCR. *Applied Environmental Microbiology* **72**: 5957-5962.

Katoh, K., Misawa, K., Kuma, K.I., & Miyata, T. (2002). MAFFT: a novel method for rapid multiple sequence alignment based on fast Fourier transform. *Nucleic acids research* **30**: 3059-3066.

Kearse, M., Moir, R., Wilson, A., Stones-Havas, S., Cheung, M., Sturrock, S., & Thierer, T. (2012). Geneious Basic: an integrated and extendable desktop software platform for the organization and analysis of sequence data. *Bioinformatics* **28**: 1647-1649.

Kim, I.S., Ekpeghere, K.I., Ha, S.Y., Kim, B.S., Song, B., Kim, J.T., Kim, H.G., Koh, S.C. (2014). Full-scale biological treatment of tannery wastewater using the novel microbial consortium BM-S-1. J. *Environ. Sci. Health Part A Tox. Hazard. Subst. Environ. Eng.* **49**: 355–364.

Knowles, R. (1982). Denitrification. *Microbiological reviews* **46**: 43.

Letunic, I. & Bork, P. (2016). Interactive tree of life (iTOL) v3: an online tool for the display and annotation of phylogenetic and other trees. *Nucleic acids research* **44**: 242-245.

Liu, Y., Liu, Y., Zhou, H., Li, L., Zheng, J., Zhang, X., & Pan, G. (2016). Abundance, composition and activity of denitrifier communities in metal polluted paddy soils. *Scientific reports* **6**.

Luedke, R.G. (1996) Geologic Map of the Ophir Quadrangle, San Juan, San Miguel, and Dolores Counties, Colorado. U.S. Geological Survey Geologic Quadrangle Series GQ-1760.

Martens-Habbena W., Berube P.M., Urakawa, H., de la Torre, J.R., & Stahl D.A. (2009). Ammonia oxidation kinetics determine niche separation of nitrifying Archaea and Bacteria. *Nature* **461**: 976–979.

Méndez-García, C., Peláez, A.I., Mesa, V., Sánchez, J., Golyshina, O.V., & Ferrer, M. (2015). Microbial diversity and metabolic networks in acid mine drainage habitats. *Frontiers in microbiology* **6**: 475.

McKnight, D.M. & Bencala, K.E. (1990). The Chemistry of Iron, Aluminum, and Dissolved Organic Material in Three Acidic, Metal-Enriched, Mountain Streams, as Controlled by Watershed and in-Stream Processes. *Water Resources Research*. **26**: 3087-3100.

Mosier, A.C. & Francis, C.A. (2010). Denitrifier abundance and activity across the San Francisco Bay estuary. *Environmental Microbiology Reports* **2***:* 667-676.

Mosier, A.C., Miller, C.S., Frischkorn, K.R., Ohm, R.A., Li, Z., LaButti, K., Lapidus, A., Lipzen, A., Chen, C., Johnson, J., Lindquist, E.A., Pan, C., Hettich, R.L., Grigoriev, I.V., Singer, S.W., & Banfield, J.F. (2016). Fungi contribute critical but spatially varying roles in nitrogen and carbon cycling in acid mine drainage. *Frontiers in microbiology* **7**.

Nägele, W., & Conrad, R. (1990). Influence of pH on the release of NO and N2O from fertilized and unfertilized soil. *Biology and Fertility of Soils* **10**: 139-144.

Nash, J. T. (2002). Hydrogeochemical investigations of historic mining districts, Central Western Slope of Colorado, including influence on surface-water quality. US Department of the Interior, US Geological Survey (USGS).

Neubert, J.T. (2002) History, Geology, and Environmental Setting of Selected Mines Near Ophir, Uncompahgre National Forest, San Miguel County, Colorado. *Colorado Geological Survey*.

Parkin, T.B., Sexstone, A.J., & Tiedje, J.M. (1985). Adaptation of denitrifying populations to low soil pH. *Applied and Environmental Microbiology* **49**: 1053-1056.

Palmer, K., & Horn, M.A. (2015). Denitrification activity of a remarkably diverse fen denitrifier community in Finnish Lapland is N-oxide limited. *PloS one* **10**: 123.

Philippot, L. (2002). Denitrifying genes in bacterial and archaeal genomes. *Biochimica et biophysica acta (BBA)-Gene structure and expression* **3**: 355-376.

Price, M.N., Dehal, P.S., & Arkin, A.P. (2010). FastTree 2–approximately maximum-likelihood trees for large alignments. *PloS one* **5**: 9490.

Ramanathan, B. (2016). *Abundance and diversity of nitrifying microbes in sediments impacted by acid mine drainage*. University of Colorado at Denver.

Roane, T., & Lantz, M. (2016). Microbial Uses in the Remediation of Metal-Impacted Soils. In *Manual of Environmental Microbiology, Fourth Edition* (pp. 5-2). American Society of Microbiology.

Sackett, J. D. (2015). *Comparative microbial ecology of sediment-associated microbial communities from anthropogenically and endogenously metal impacted systems*. University of Colorado at Denver.

Saeed, A., Bhagabati, N., Braisted, J., Sturn, A., & Quackenbush, J. (2003). TIGR MeV Multiexperiment Viewer. *The Institute for Genomic Research*.

Sakadevan, K., Zheng, H., & Bavor, H.J. (1999). Impact of heavy metals on denitrification in surface wetland sediments receiving wastewater. *Water Science and Technology* **40**: 349-355.

Saleh-Lakha, S., Shannon, K.E., Henderson, S.L., Goyer, C., Trevors, J.T., Zebarth, B.J., & Burton, D.L. (2009). Effect of pH and temperature on denitrification gene expression and activity in Pseudomonas mandelii. *Applied and environmental microbiology* **75**: 3903-3911.

Sandaa, R.A., Torsvik, V., & Enger, Ø. (2001). Influence of long-term heavy-metal contamination on microbial communities in soil. *Soil Biology and Biochemistry* **33**: 287-295.

Santoro, A.E., Boehm, A.B., & Francis, C.A. (2006). Denitrifier community composition along a nitrate and salinity gradient in a coastal aquifer. *Applied and Environmental Microbiology* **72**: 2102-2109.

Seitzinger, S., Harrison, J. A., Böhlke, J. K., Bouwman, A. F., Lowrance, R., Peterson, B., Tobias, C., & Van Drecht, G. (2006). Denitrification across landscapes and waterscapes: a synthesis. *Ecological Applications* **6:** 2064-2090.

Shapleigh, J.P. (2013). Denitrifying prokaryotes. In *The prokaryotes* (pp. 405-425). Springer Berlin Heidelberg.

Šimek, M., Jíšová, L., and Hopkins, D.W. (2002) What is the so-Called Optimum pH for Denitrification in Soil?. *Soil Biology and Biochemistry* **34**:1227-34.

Smith, J.M., & Ogram, A. (2008). Genetic and functional variation in denitrifier populations along a short-term restoration chronosequence. *Applied and environmental microbiology* **74**: 5615-5620.

Sobolev, D. & Begonia, M. (2008). Effects of heavy metal contamination upon soil microbes: lead-induced changes in general and denitrifying microbial communities as evidenced by molecular markers. *International journal of environmental research and public health* **5**: 450-456.

Ter Braak, C. (1985). Canonical correspondence analysis: a new eigenvector technique for multivariate direct gradient analysis. *Ecology* **67**: 1167-1179.

Thamdrup, B. (2012) New Pathways and Processes in the Global Nitrogen Cycle. *Annual Review of Ecology, Evolution, and Systematics* **43**: 407-28.

Throbäck, I.N., Enwall, K., Jarvis, Å., & Hallin, S. (2004). Reassessing PCR primers targeting nirS, nirK and nosZ genes for community surveys of denitrifying bacteria with DGGE. *FEMS microbiology ecology* **49**: 401-417.

Throbäck, I.N., Johansson, M., Rosenquist, M., Pell, M., Hansson, M., & Hallin, S. (2007). Silver (Ag+) reduces denitrification and induces enrichment of novel nirK genotypes in soil. *FEMS Microbiology Letters* **270**: 189-194.

Wallenstein, M.D., Myrold, D.D., Firestone, M., & Voytek, M. (2006). Environmental Controls on Denitrifying Communities and Denitrification Rates: Insights from Molecular Methods. *Ecological Applications* **16**: 2143-2152.

Wei, W., Isobe, K., Nishizawa, T., Zhu, L., Shiratori, Y., Ohte, N., Koba, K., Otsuka, S., & Senoo, K. (2015). Higher diversity and abundance of denitrifying microorganisms in environments than considered previously. *The ISME journal* **9**: 1954.

Wijler, J. & Delwiche, C.C. (1954) Investigations on the denitrifying process in soil. *Plant and Soil* **5**: 155–169.

Zumft, W.G. (1997) Cell biology and molecular basis of denitrification. *Microbiology and Molecular Biology Review* **61**: 533–616.

APPENDIX

SUPPLEMENTAL TABLES AND FIGURES

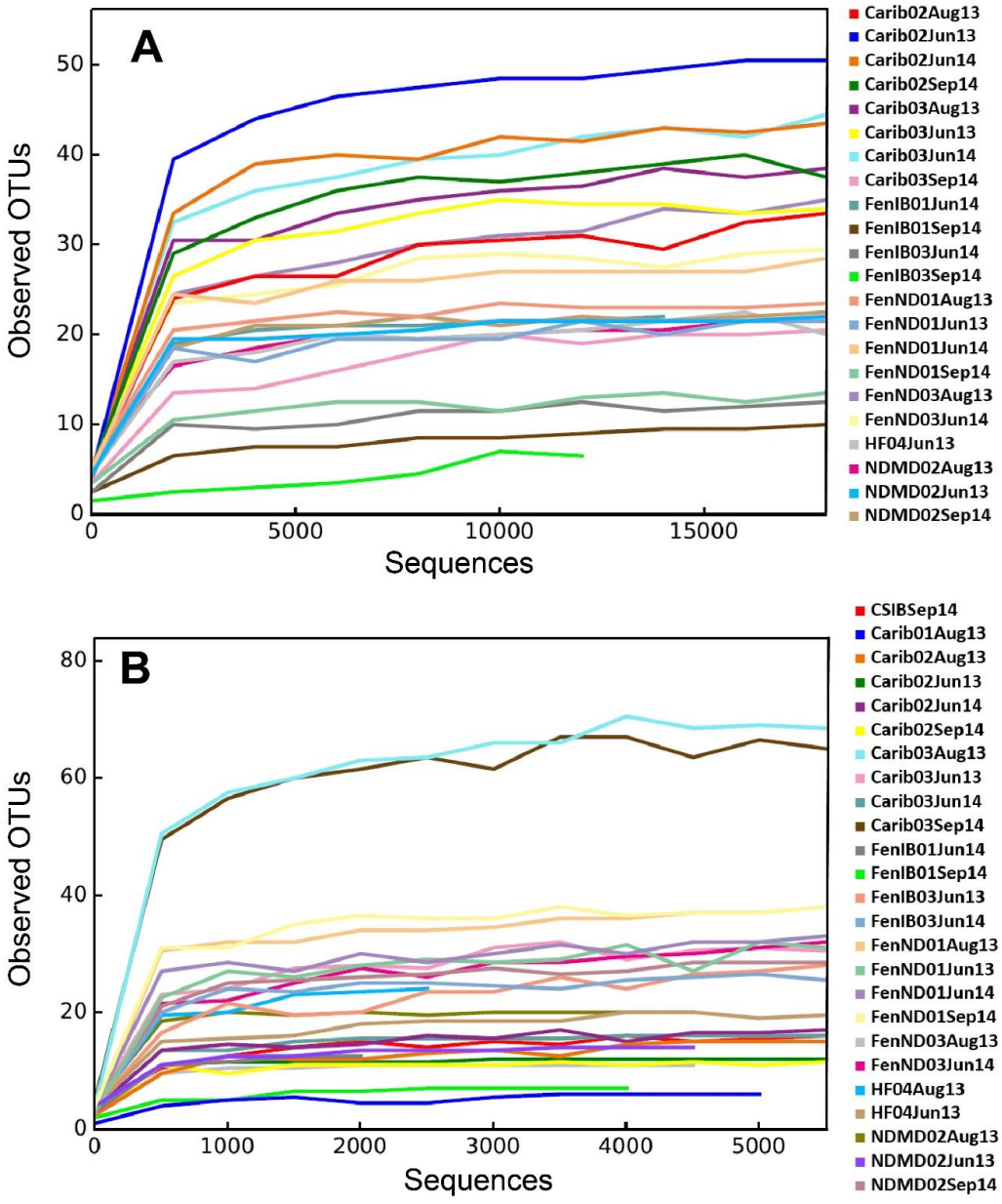

Figure S1: Rarefaction curves for *nirK* gene sequences across all samples (Panel A); samples containing fewer than 13,000 reads were excluded from analysis. Rarefaction curves for *nirS* gene sequences across all samples (Panel B); samples containing fewer than 1,000 reads were excluded from analysis.

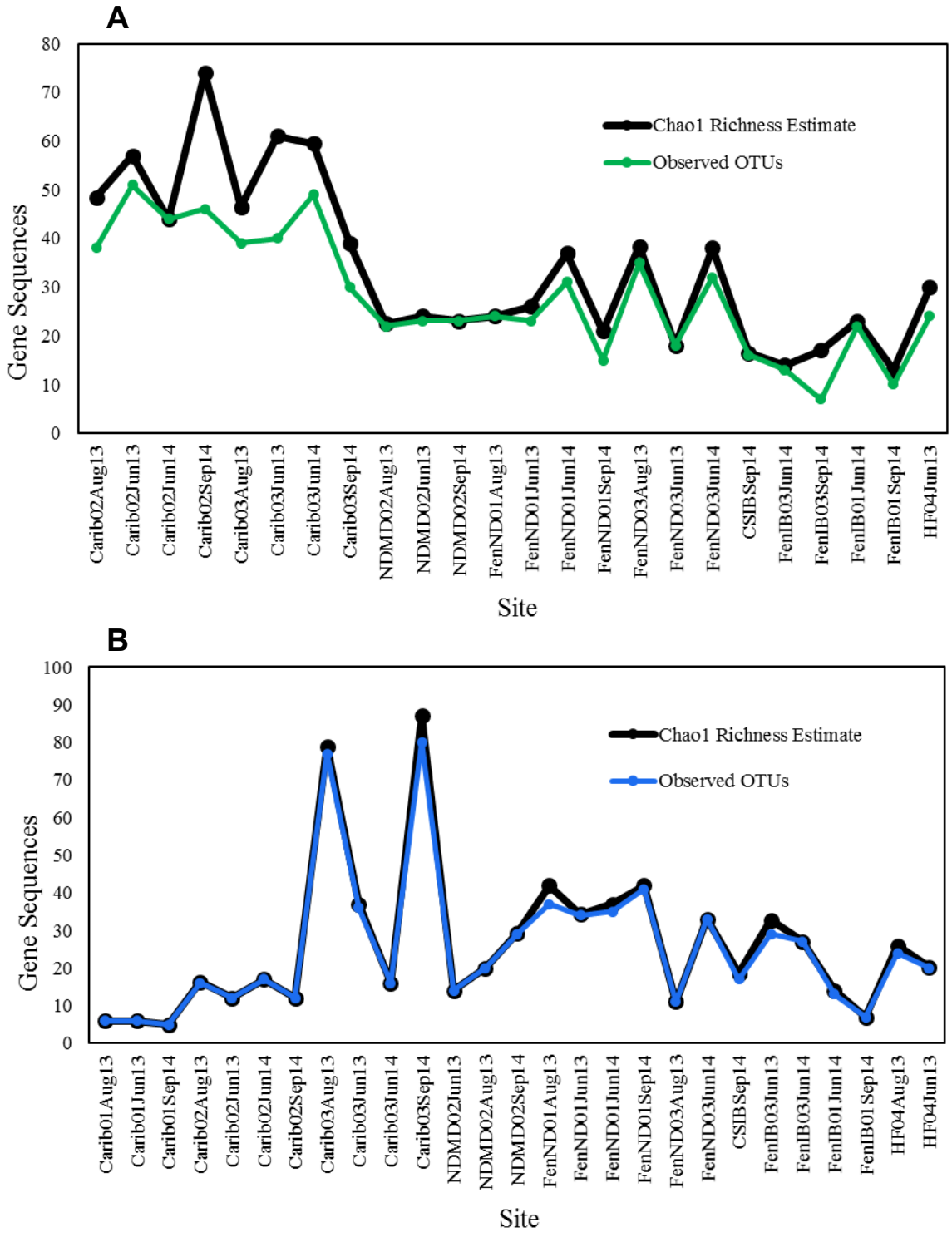

Figure S2: Number of observed OTUs and Chao1 richness estimates for *nirK* (Panel A) and *nirS* (Panel B) gene sequences across all sample sites.

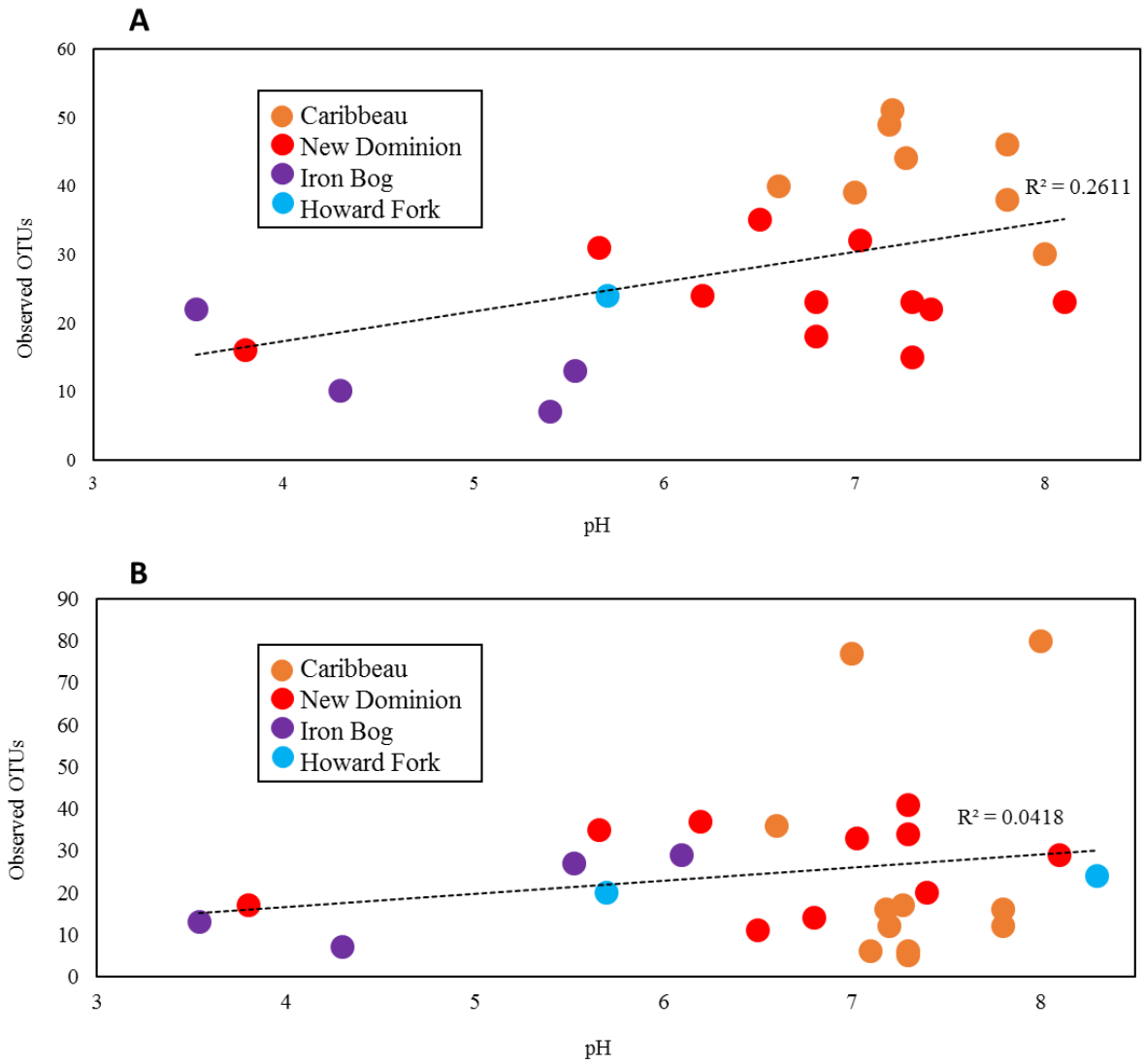

Figure S3: Comparison between the number of observed *nirK* OTUs (panel A) and the number of observed *nirS* OTUs (panel B) to the sediment pH at each site. Samples within the four regions are indicated by separate colors.

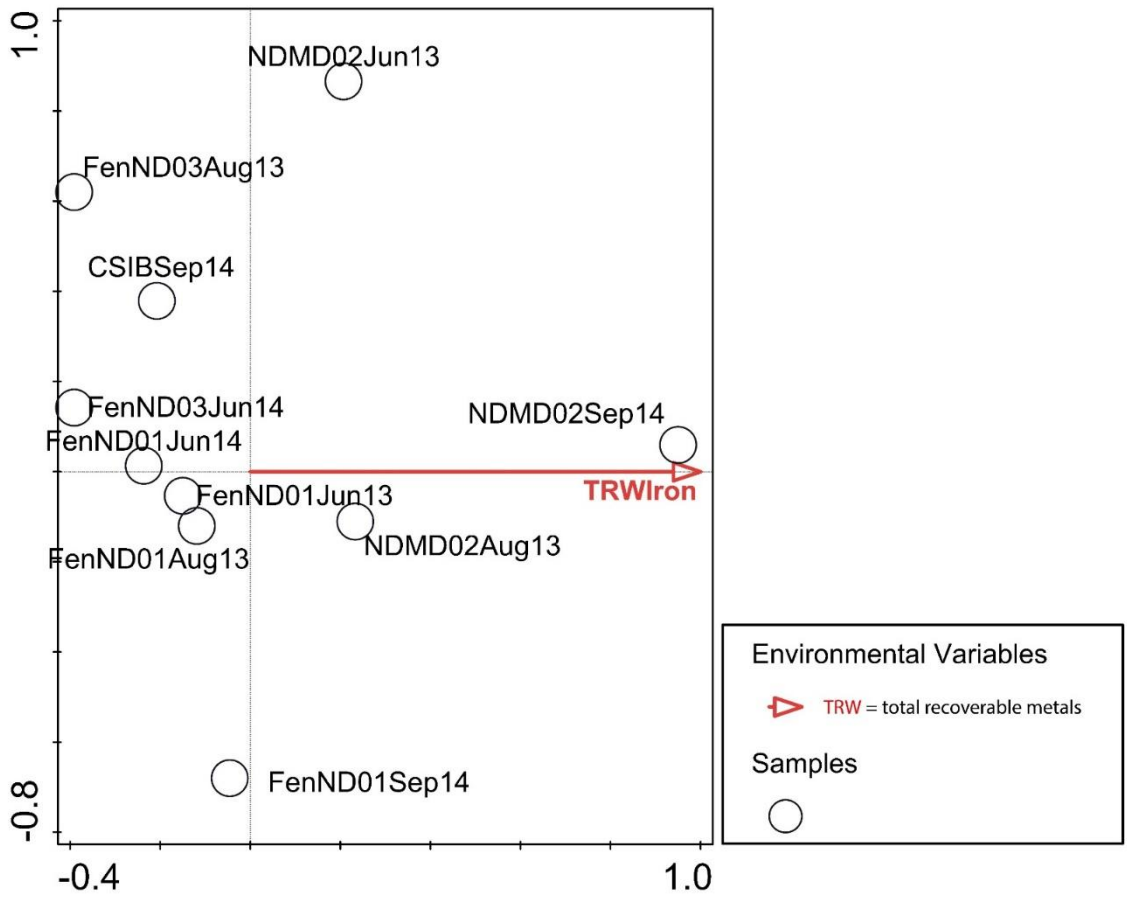

Figure S4: Canonical Correspondence Analysis (CCA) of relative gene abundance of *nirS* gene sequences for individual samples within the New Dominion region. TRW Iron significantly correlated (Bonferroni corrected p-value <0.05) to the distribution of relative gene abundance.

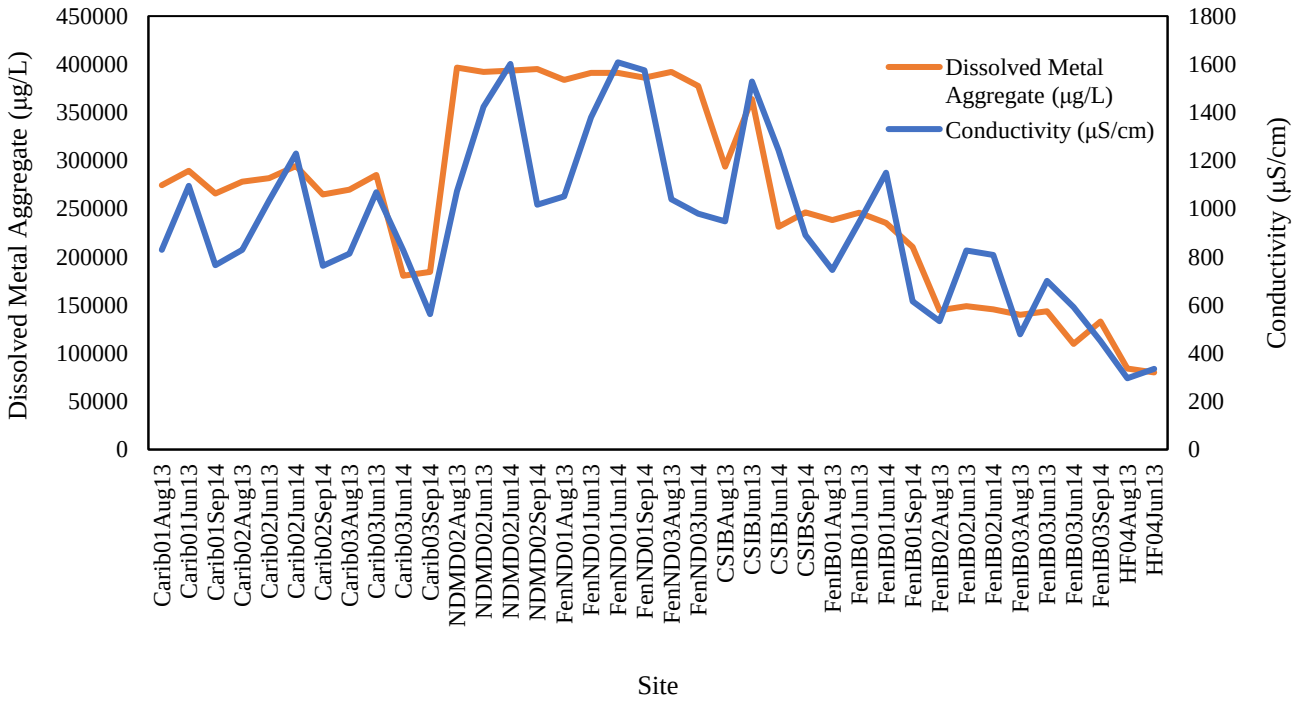

Figure S5. Comparison of conductivity to the sum of all dissolved metals at each site with a Pearson correlation coefficient of 0.83 and an R^2 value of 0.68.